Endocranial anatomy and life habits of the Early Triassic archosauriform Proterosuchus fergusi

Brown, Emily; Butler, Richard; Ezcurra, Martin; Bhullar, Bhart-Anjan; Lautenschlager, Stephan

Endocranial anatomy and life habits of the Early Triassic archosauriform *Proterosuchus fergusi*

EMILY E. BROWN[1*], RICHARD J. BUTLER[1], MARTÍN D. EZCURRA[1,2], BHART-ANJAN S. BHULLAR[3], STEPHAN LAUTENSCHLAGER[1*]

[1]School of Geography, Earth and Environmental Sciences, University of Birmingham, Birmingham, United Kingdom

[2]Sección Paleontología de Vertebrados, CONICET−Museo Argentino de Ciencias Naturales "Bernardino Rivadavia", Buenos Aires, Argentina

[3]Department of Geology and Geophysics, Yale University, New Haven, Connecticut, USA

*Corresponding authors: emilyb62@hotmail.com, s.lautenschlager@bham.ac.uk

Abstract: Proterosuchids are an important group of carnivorous basal archosauriforms characterised by a bizarre and enigmatic downturned premaxilla that overhangs the lower jaw. They are particularly significant because they radiated in the immediate aftermath of the Permian−Triassic mass extinction, and represent one of the best known 'disaster taxa' following that event. While traditionally considered semi-aquatic, recent histological studies and geological data have suggested that they more likely inhabited terrestrial environments. By utilising computed tomographic (CT) data, we virtually reconstruct the brain endocast and endosseous labyrinths of two adult specimens of *Proterosuchus fergusi* from the earliest Triassic of South Africa, in an attempt to understand its life habits within the context of basal

26   archosauriform evolution. Endocasts reveal that the brain cavity is tubular in shape and the

27   endosseous labyrinths are highly pyramidal. The angle of the lateral semi-circular canal

28   suggests that *P. fergusi* naturally held its head upwards ~17°, while the length of the cochlear

29   duct suggests its auditory abilities were specialised towards low-frequency sounds.

30   Furthermore, beam theory analysis suggests that the rostrum of *P. fergusi* is highly resistant to

31   both bending and torsion when compared to modern crocodilians, although this resistance is

32   neither enhanced or reduced by the overhanging premaxilla. Comparative anatomical analyses

33   suggest *P. fergusi* was likely a semi-aquatic, generalist apex predator capable of surviving the

34   harsh environmental perturbations of the Early Triassic.

35

36   KEYWORDS: Archosauriformes, endocranial anatomy, brain cavity, semi-circular canals,

37   digital reconstruction, Early Triassic

38

39

40   The end-Permian mass extinction is thought to have resulted in the loss of up to ~96% of life

41   on Earth, including ~70% of terrestrial vertebrates (Raup 1979; Jablonski 1995; Benton &

42   Twitchett 2003; Chen & Benton 2012). Despite the desolate greenhouse conditions of the

43   Early Triassic, the opening up of new ecosystems and niches allowed for an adaptive

44   radiation of surviving clades (Chen & Benton 2012; Viglietti *et al.* 2013; Foth *et al.* 2016;

45   Ezcurra & Butler 2018). Originating in the middle–late Permian, the diapsid clade

46   Archosauriformes successfully gained a foothold in the Early Triassic world, and gave rise to

47   groups that would go on to dominate in the Mesozoic (e.g. crocodylomorphs, dinosaurs,

48   pterosaurs) as well as continuing to make up a considerable portion of the modern fauna (e.g.

49   birds, crocodylians) (Ezcurra *et al.* 2014; Pinheiro *et al.* 2016; Ezcurra & Butler 2018).

50   The basal archosauriform group Proterosuchidae, characterised by an enigmatic

51 downturned premaxilla that overhangs the anterior margin of the lower jaw, is often referred

52 to as a 'disaster' clade that thrived for a geologically short interval following the end-Permian

53 extinction (e.g. Ezcurra 2016; Button *et al.* 2017). The clade attained a near cosmopolitan

54 distribution, with specimens found in China, India, and South Africa (Ezcurra *et al.* 2013;

55 Ezcurra 2016). The type species of this clade, *Proterosuchus fergusi* Broom 1903, is known

56 from the *Lystrosaurus* Assemblage Zone (AZ) of the Karoo Supergroup of South Africa.

57 Although well sampled, with eleven highly informative specimens, many aspects of the

58 species' life habits and functional morphology are still unknown (Ezcurra & Butler 2015a).

59 Traditionally, *P. fergusi* was considered semi-aquatic due to its superficial similarity to

60 modern crocodylians and the then-presumed wet climate of the Early Triassic Karoo Basin

61 (Broili & Schröder 1934; Tatarinov 1961; Reig 1970). Further evidence for an aquatic affinity

62 included the predominately horizontal orientation of vertebral zygapophyses, allowing for

63 lateral flexure of the body, which crocodiles use to propel themselves through the water

64 (Cruickshank 1972).

65   However, proterosuchid ecology has since been disputed, with several authors

66 suggesting a more terrestrial life habit (Cruickshank 1972; Welman 1998; Botha-Brink &

67 Smith 2011). Cruickshank (1972) and Welman (1998) noted the lack of dorsally positioned

68 external nares, which are an adaptation typical of aquatic and semi-aquatic diapsids such as

69 plesiosaurs, mosasaurs, phytosaurs and crocodylians (Sereno 1991; Nesbitt *et al.* 2009).

70 Cruickshank (1972) also noted the presence of well-ossified limbs, carpus and tarsus, and the

71 vertical orientation of the occipital elements, and suggested *P. fergusi* was largely terrestrial.

72 Furthermore, Botha-Brink & Smith (2011) combined sedimentological data and an

73 osteohistological analysis of several *P. fergusi* limb bones, which provided no evidence of

74 osteological specialisation to aquatic life (such as pachyosteosclerosis or osteoporosis), to

75   suggest a terrestrial mode of life for this species. However, palaeohistological analyses are not

76   always accurately indicative of ecology, with, for example, a similar study finding no aquatic

77   osteological specialisations in the marine teleosaurids, *Steneosaurus* and *Teleosaurus* (Hua &

78   De Buffrenil 1996).

79   *Proterosuchus fergusi* is both the earliest new tetrapod following the onset of the

80   Triassic and the best-sampled basal archosauriform species from the Karoo Basin (Smith &

81   Botha 2005; Botha-Brink & Smith 2011; Smith *et al.* 2012). Therefore, consensus on the life

82   habits of this species is crucial to understanding the faunal recovery following the end-

83   Permian mass extinction. While the neuroanatomy and inner ear morphology of archosaurs

84   have been extensively studied, non-archosaurian archosauromorphs have been widely

85   neglected, in part due to their comparatively poor fossil record. To date, the brain endocast of

86   only one basal archosauriform has been described in the literature, the proterochampsian

87   *Tropidosuchus romeri* (Trotteyn & Paulina-Carabajal 2016). Several basal archosauriform

88   endosseous labyrinths have been virtually reconstructed (Sobral *et al.* 2016a; Trotteyn &

89   Paulina-Carabajal 2016); however, none are complete.

90   This study presents the first in-depth assessment of the endocranial anatomy of the

91   basal archosauriform *P. fergusi*. Based on data from the endocranial reconstructions, we

92   further discuss the life habits and ecology of *P. fergusi* and implications for the early

93   evolution of Archosauriformes.

94

95   **METHODS**

96   *Specimens*

97   The skulls of two specimens of *Proterosuchus fergusi* were used in this study, RC 846

98   (Rubidge Collection, Wellwood, Graaff-Reinet, South Africa) and SNSB-BSPG 1934 VIII

99   514 (Staatliche Naturwissenschaftliche Sammlungen Bayerns/Bayerische Staatssammlung für

100   Paläontologie und Geologie, Munich, Germany) (Fig. 1). Both specimens are large adults

101   from the *Lystrosaurus* AZ of the Karoo Basin of South Africa (Ezcurra & Butler 2015b). The

102   left side of SNSB-BSPG 1934 VIII 514 is nearly complete, but the right side has been subject

103   to severe deformation and loss of information (Fig. 1B-C). The specimen also previously

104   underwent substantial reconstruction in an attempt to adhere disarticulated and fractured

105   elements, especially in the premaxillary region (Broili & Schröder 1934). RC 846 is far more

106   complete but the skull is moderately transversely compressed and its posterior region has

107   been moderately crushed. The premaxilla is also largely complete and articulated in this

108   specimen.

109

110   *Scanning*

111   RC 846 was CT scanned at the University of Texas High-Resolution X-ray CT Facility

112   Archive. The braincase of RC 846 is disarticulated from the rest of the skull, allowing it to be

113   µCT scanned separately (hereafter 'RC 846 µCT'). SNSB-BSPG 1934 VIII 514 was CT

114   scanned at the Klinikum rechts der Isar (Munich). Datasets consist of 548 coronal slices (1024

115   x 1024 pixels, voxel size 0.211 mm) for RC 846, 457 oblique (~15° ventroposterior deviation)

116   coronal slices (1024 x 1024 pixels, voxel size 0.117 mm) for RC 846 µCT, and 1229 coronal

117   slices (768 x 526 pixels, voxel size 0.5 mm) for SNSB-BSPG 1934 VIII 514. Original CT

118   data for SNSB-BSPG 1934 VIII 514 are available in the Dryad Digital Repository:

119   https://datadryad.org/review?doi=doi:10.5061/dryad.XXXX. Original CT data for RC 846 are

120   archived at Yale University and are available from B.-A.S. upon request.

121

122   *Virtual Endocast Construction*

123   The CT data were imported into SPIERSedit (2.20, www.spiers-software.org). Areas of

124   interest such as the endosseous labyrinths, braincase and nerves were manually segmented

125   using the Masks and Curves tools following Balanoff *et al.* (2016) (see Brown *et al.* 2019, fig.

126   S1). Interactive 3D PDFs of the endocranial reconstructions are provided as supplementary

127   information.

128

Morphometric Outline Analysis

130   Elliptical Fourier analysis (EFA) was used in this study to quantify the morphological

131   variability of brain and inner ear endocasts among diapsid groups. EFA statistically compares

132   the co-ordinates of complex 2D shapes or outlines. EFA is very versatile as it can be used to

133   compare shapes where homologous features are hard to distinguish (Crampton 1995). As a

134   result, EFA is widely used in both the palaeontological and biological sciences to study

135   interspecific (e.g. Crampton 1995; Bonhomme *et al.* 2013; Vidal *et al.* 2014; Lautenschlager

136   2014; Lautenschlager *et al.* 2018) and intraspecific (e.g. Polihronakis 2006; Ramajo *et al.*

137   2013) anatomical variation.

138

Brain Outline Preparation. An outline of the most complete *Proterosuchus fergusi*

140   endocranial reconstruction (RC 846) was drawn in Adobe Illustrator (CS5, www.adobe.com).

141   The brain cavities of 69 extinct and extant archosauriforms compiled from the literature were

142   also outlined in Adobe Illustrator. For consistency, the left lateral view was always used. If

143   unavailable, the right lateral view was reversed. Natural, artificial (e.g. latex) and virtual

144   endocasts were used for comparative taxa. Brain cavity outlines and taxonomic information of

145   all comparative taxa are available in Table S1. Outline co-ordinates were digitised in tpsDig2

146   (v2.31, Rohlf 2010) as 1000 x/y pairs.

147

148   *Inner Ear Outline Preparation.* The inner ear is divided into two regions, both with different

149   functions: the semi-circular canals are part of the vestibular region, responsible for balance

150   and co-ordination; whereas the endosseous cochlear duct (ECD) is part of the auditory

151   system, responsible for hearing. To determine whether these features have evolved separately

152   the inner ear was outlined and analysed both with and without the ECD. Analysis without the

153   ECD also allowed the inclusion of the basal archosauriform *Euparkeria capensis,* for which

154   the ECD could not be reconstructed (Sobral *et al.* 2016a). Prior to this study, *E. capensis* was

155   the only non-archosaurian archosauriform for which three articulated semi-circular canals had

156   been virtually reconstructed.

157   For this analysis, a computerised outline procedure was used. Images of the left

158   labyrinth from extinct and extant diapsid taxa (n = 94, with ECD; n = 99, without ECD) were

159   collected from the literature. These were then converted into binary images by altering the

160   threshold in Adobe Photoshop (CS5, www.adobe.com). At this stage for the analysis

161   excluding the ECD, the polygonal lasso tool was used to select and remove the ECD. Images

162   were then vectorised using the 'Live Trace' tool in Adobe Illustrator before using the expand

163   tool to make the vector editable. The 'Outline Stroke' tool was then used to create a

164   computer-generated outline. All endosseous labyrinths were outlined in lateral view. If the left

165   labyrinth was unavailable, the right labyrinth was reversed. Inner ear outlines and taxonomic

166   information of all comparative taxa are available in the supplementary information. Co-

167   ordinates for the outlines were digitised in tpsDig2 as 1000 x/y pairs for outlines with the

168   ECD and 750 x/y pairs for outlines without the ECD.

169

170   *Elliptical Fourier Analysis*. Outline co-ordinates were analysed respectively in PAST

171   (v3.19, Hammer *et al.* 2001) using EFA. Outlines were smoothed ten times to eliminate pixel

172   noise, and 23 Fourier harmonics were found to describe the outlines of all sampled taxa

173   sufficiently (average Fourier power > 99%). A Procrustes superimposition was performed

174   before undergoing principal component analysis (PCA). Taxa were assigned to a phylogenetic

175   group and broad ecological group (aquatic, semi-aquatic, terrestrial) (see Table S1). To test

176   whether morphological variation was significantly different between group variables

177   (ecological and phylogenetic) the non-parametric one-way PERMANOVA test was used with

178   10,000 permutations. Due to the ambiguity surrounding the ecology of *Proterosuchus fergusi*,

179   this taxon was excluded from analyses between ecology.

180

181

182   *Morphometric Landmark Analysis*

183   This analysis is an iteration of that used by Yi & Norell (2015), Neenan *et al.* (2017) and

184   Neenan *et al.* (2019) to compare the endosseous labyrinths of extant snakes, extinct

185   sauropterygians and *Massospondylus* individuals, respectively. However, unlike those

186   mentioned this analysis compares each of the different semi-circular canals (anterior semi-

187   circular canal, ASC; lateral semi-circular canal, LSC; posterior semi-circular canal, PSC)

188   separately.

189   The semi-circular canals generated from RC 846 μCT and RC 846 were used for this

190   analysis. Additionally, the inner ears of comparative extinct and extant diapsid taxa (n=37,

191   ASC; n=51, LSC; n=35, PSC) were sourced from the literature. The left labyrinth was

192   selected for this analysis due to its relative availability, but if unavailable the right labyrinth

193   was reversed.

194   Screenshots of each semi-circular canal were taken perpendicular to the plane to

195   remove perspective skew. The external and internal surface of each canal was outlined in

196   Adobe Illustrator using the automated approach described above. The dashed line stroke tool

197   was used to find 21 equally-spaced points along the external surface of each canal and 11

198   along the inner surface of each canal. These dashed lines were used as a reference point for

199   accurate and consistent landmark placing. The outlines with their reference points were

200   imported into tpsDig2 and landmarks were placed in a designated order. Co-ordinates were

201   exported from tpsDig2 and imported into MorphoJ (v1.06d,

202   www.flywings.org.uk/morphoj_page.htm). To mitigate the effects of varying orientation,

203   sizing, and distance between landmarks of different canals, a Procrustes superimposition was

204   performed (following Neenan *et al.* 2017). Principal component analysis was run and plotted

205   to show geometric variability. A canonical variate analysis (CVA) was used to test the

206   morphological variance of diapsid semi-circular canals between different phylogenetic and

207   ecologic groupings, respectively. Due to the ambiguity surrounding the ecology of

208   *Proterosuchus fergusi*, this taxon was excluded from analyses between ecology.

209

210   *Head posture*

211   The orientation of the LSC ('horizontal semi-circular canal') has been widely used to infer the

212   head posture of fossil taxa (Rogers 1998; Witmer *et al.* 2003; Sampson & Witmer 2007;

213   Sereno *et al.* 2007; Witmer *et al.* 2008; Witmer & Ridgely 2009; Neenan & Scheyer 2012;

214   Benoit *et al.* 2017), however not without criticism (Hullar 2006; Taylor *et al.* 2009; Marugán-

215   Lobón *et al.* 2013). As part of the vestibular system, it is thought that many species habitually

216   hold their LSC in a horizontal orientation (Lebedkin 1924; de Beer 1947). For example, the

217   LSC orientation in the basal sauropterygian *Placodus gigas* suggests that it was down tilted

218   ~20° (Neenan & Scheyer 2012). Neenan & Scheyer (2012) suggested that the downturned

219   head posture was adapted for aquatic herbivory and concluded that *Pl. gigas* was fully

220   adapted for aquatic life despite being one of the most basal sauropterygians.

221

222   *Orientation of the lateral semi-circular canal.* Screenshots of the isolated LSC and whole

223   skull (skull at 75% opacity) were taken in SPIERS View to show both the skull and LSC. The

224   orientation of each LSC was measured in ImageJ using the angle tool. Lateral semi-circular

225   canals reconstructed from RC 846 μCT were excluded from this analysis because the scans

226   only contained the braincase region. Often in these analyses, the 'horizontal' is measured as

227   the bottom surface of the dentary (e.g. Witmer & Ridgely 2009). However, as both of the

228   mandibles in RC 846 and SNSB-BSPG 1934 VIII 514 are significantly deformed, the

229   maxillary tooth-line was used instead as the horizontal plane. The left and right LSC planes

230   were measured separately. The mean average was calculated from all four values.

231

232   *Auditory Abilities*

233   The mean hearing frequency and hearing range of *Proterosuchus fergusi* were estimated

234   following methods from Walsh *et al.* (2009). The endosseous cochlear duct (ECD) length is

235   considered a proxy of auditory ability. The study from Walsh *et al.* (2009) used a linear

236   regression of scaled ECD length and sensitivity data of extant avian and reptilian taxa to

237   estimate the auditory abilities of several extinct Aves. This has since been repeated with the

238   Early Jurassic marine crocodylomorph *Steneosaurus* cf. *gracilirostris* (Brusatte *et al.* 2016)

239   and with the basal eusuchian *Lohuecosuchus megadontos* (Serrano-Martínez *et al.* 2018). As

240   individuals can typically only hear within their own vocal range, estimations of auditory

241   acuity can be informative regarding vocality (Narins *et al.* 2004). Vocality and auditory

242   ability are also considered to be indicators of sociality and cognitive ability, since larger more

243   complex groups require better communicative skills to work together efficiently (Blumstein &

244   Armitage 1997; Freeberg *et al.* 2012; Freeberg & Krams 2015; Sewall 2015). This is

245   corroborated by Walsh *et al.* (2009) who found longer ECD length to be significantly

246   correlated with animals living in larger group sizes.

247

248   *Regressions.* This study uses ECD length (scaled to basicranial length) and hearing sensitivity

249   data derived from Walsh *et al.* (2009). Additional data on the hearing sensitivity of extant

250   archosaurs was also collected from the literature (Corfield *et al.* 2013; Bonke *et al.* 2015)

251   giving a total of 26 comparative taxa. RC 846 produced the most complete endocast and so

252   was the only proterosuchid specimen used in the analysis. The ECD length of RC 846 was

253   measured and scaled to the basicranial length (measured from the basisphenoid-presphenoid

254   suture to the caudal-most tip of the occipital condyle, S. Walsh 2018 pers. comm.).

255   All scaled ECD lengths were log-transformed. Log-scaled ECD length for extant taxa

256   was plotted against respective mean hearing and hearing range data. Both an ordinary least

257   squares linear regression and a phylogenetic generalized least square regression were

258   calculated for this analysis. These regression lines were used to predict mean hearing and

259   hearing range for *Proterosuchus fergusi* based on the scaled and log-transformed ECD length.

260   Analyses were conducted using R (RStudio v1.1.423, www.rstudio.com). The R packages ape

261   (5.3, Paradis *et al.* 2004), geiger (2.0.6.1, Harmon *et al.* 2007), nlme (3.1-137, Pinheiro *et al.*

262   2018) and phytools (0.6-60, Revell 2012) were used to calculate the phylogenetic generalized

263   least square (PGLS) regression with a Brownian motion model of trait evolution. The analysis

264   used a phylogenetic tree of all comparative taxa generated from http://timetree.org/.

265

266   *Snout Beam Analysis*

267   Beam theory was used to investigate the relative rostral resistance of *Proterosuchus fergusi* to

268   bending and torsion. Beam theory calculates the potential bending of an object based on the

269   density and distribution of material around the neutral axis (the centre of an object, where

270   there is no tension or compression) (Therrien *et al.* 2005; Cuff & Rayfield 2013). For

271   example, a hollow tube is more resistant to bending than an infilled tube because material is

272   distributed further from the neutral axis. To test the biomechanical resistance of rostra and

273   lower jaws, this technique has been previously applied to a range of fossil taxa (Therrien *et al.*

274   2005; Cuff & Rayfield 2013; Foffa *et al.* 2014).

275

276   *Slice Preparation.* Slices were chosen along the rostrum at intervals. The first 20% of the

277   rostrum was sliced at intervals of 2% as the premaxillary area is of specific interest in

278   *Proterosuchus fergusi*. Due to the extent of the overhanging premaxilla in *P. fergusi*, a

279   straight beam may not be considered appropriate for this taxon. Therefore, for the rostral 20%

280   of the snout both a straight beam and curved beam were used in the analysis for *P. fergusi*.

281   For the curved beam analysis, the rostrum of *P. fergusi* was sliced at intervals of 4% rather

282   than 2% to prevent slices overlapping. The latter 80% of the rostrum was sliced at intervals of

283   10%. RC 846 was used for this analysis because the premaxillae of SNSB-BSPG 1934 VIII

284   514 have undergone significant reconstruction and may not represent the true original shape

285   (Fig. 1). As RC 846 was scanned along the coronal axis, the raw CT slices could be used in

286   this analysis.

287   For comparative analysis, five extant taxa were chosen: four pseudosuchians, *Alligator*

288   *mississippiensis* (American alligator), *Crocodylus moreletii* (Morelet's crocodile), *Crocodylus*

289   *rhombifer* (Cuban crocodile) and *Tomistoma schlegelii* (false gharial); and one

290   actinopterygian, *Atractosteus spatula* (alligator gar). *Atractosteus spatula* was included

291   because of the slight overhang of the premaxilla, similar to that of *P. fergusi*.

292   The skull of *A. spatula* was downloaded as CT data from Digimorph.org. The

293   specimen was scanned along the coronal plane so slices for this analysis could be taken

294   directly from the raw CT-scans. Skulls of *C. moreletii*, *C. rhombifer*, and *T. schlegelii* were

295   downloaded as STL files from Digimorph.org. *Alligator mississippiensis* (juvenile) was

296   downloaded from Digimorph.org as CT data sliced along the horizontal plane so the raw

297   slices could not be used in this analysis. *Alligator mississippiensis* was exported from

298   SPIERSview as an STL file. These four STL files were imported into Blender (2.79a,

299   www.blender.org) and manually sliced using the Boolean Modifier tool. A visual reference

300   was used to accurately slice at the correct positions along the rostrum. All slices were

301   rendered against the same flat plane for consistency. For the curved beam analysis RC 846

302   was imported into Avizo Lite (9, Thermo Fisher Scientific) and the rotate tool was used create

303   the required slices.

304   All slices were imported into Adobe Photoshop where mandibles were manually

305   removed. Teeth can vastly increase the proportion of material in the slice, especially in

306   specimens with larger teeth (Cuff & Rayfield 2013). To standardise these effects, teeth were

307   removed and the alveoli flattened in all slices. Additionally, in *P. fergusi*, the sediment was

308   manually removed from the slices and rostrum walls were slightly corrected by

309   symmetrisation. All slices were then converted into binary images by altering the image

310   threshold.

311

312   *Second moments calculation and analysis.* Prepared slices were imported into ImageJ (1.51j8,

313   www.imagej.nih.gov/ij). The second moments of area in the dorsoventral (I_x) and

314   mediolateral (Iy) directions and the polar moment of inertia (J) were calculated using the

315   ImageJ macro, MomentMacroJ (v1.4, www.hopkinsmedicine.org/fae/mmacro.html). In an

316   additional analysis, rostra were scaled to the rostral length of *Proterosuchus fergusi* (aspect

317   ratio was maintained) to determine whether size difference influenced results (see

318   Supplementary material). All results were log transformed and plotted using R. A paired t-test

319   was computed between *P. fergusi* and comparative taxa for the entire rostrum and the first

320   anterior 20% of the rostrum both at true size and scaled size and also using both a straight and

321   curved beam.

322

RESULTS

323

324

325   *Virtual Endocast Reconstruction*

326   *Brain Cavity.* The endocranial reconstructions of *Proterosuchus fergusi* are generally linear in

327   shape and organisation (Fig. 2), similar to that of modern-day adult crocodylians (Jirak &

328   Janacek 2017). The brain cavity of *P. fergusi* is straighter than many archosauriforms

329   including erythrosuchids (Gower & Sennikov 1996), phytosaurs (Holloway *et al.* 2013;

330   Lautenschlager & Butler 2016) and many crocodylomorphs (Witmer *et al.* 2008; Witmer &

331   Ridgely 2009; Kley *et al.* 2010), but analogous to the thalattosuchians *Pelagosaurus typus*

332   and *Steneosaurus gracilirostris* (Brusatte *et al.* 2016; Pierce *et al.* 2017).

333   Due to breaks at the frontal-parietal suture in both RC 846 and SNSB-BSPG 1934

334   VIII 514, the elongate olfactory tracts typical of many archosauriforms and non-

335   archosauriform diapsids (Witmer *et al.* 2008; Witmer & Ridgely 2009; Ezcurra 2014;

336   Lautenschlager & Butler 2016; Trotteyn & Paulina-Carabajal 2016) could not be fully

337   reconstructed in *P. fergusi*. The endocast for RC 846 µCT lacks the anterior portion of the

338   olfactory region, which would lie on the ventral surface of the frontals. This region is also

339   missing in SNSB-BSPG 1934 VIII 514 due to the poor preservation of the frontals. Shallow

340   concave fossae along the ventral surface of the frontals of RC 846 allow for the partial

341   reconstruction of the dorsal surfaces of the olfactory bulbs (Fig. 2C-D). The ventral extent of

342   the bulbs cannot be determined due to the lack of constraining bones in the region. The bulbs

343   are slightly laterally expanded and rostrally taper out into two separate structures. Unlike in

344   the basal archosauromorph *Tasmaniosaurus triassicus* (Ezcurra 2014), the olfactory bulbs of

345   *P. fergusi* are exceeded in width by the cerebral hemispheres. The morphology of these bulbs

346   allows for an estimation of the size and extent of the olfactory tracts and olfactory region as a

347   whole. Compared to other archosauriforms the olfactory region is relatively short, analogous

348   to the thalattosuchian *Pelagosaurus typus* (Pierce *et al*. 2016), but considerably larger than the

349   ornithosuchid *Riojasuchus tenuisceps* (Baczko & Desojo 2016).

350   The forebrain is bulbous and horizontal while the mid-brain is more anteroventrally

351   directed. The floccular lobes are relatively small and do not extend through the anterior semi-

352   circular canal, unlike in many archosaurs (e.g. Witmer & Ridgely 2009; Lautenschlager *et al*.

353   2012; Lautenschlager & Butler 2016). The hind brain is mediolaterally narrow, especially

354   between the endosseous labyrinths, but expands ventrally more than other parts of the

355   braincase. Ventral to the hindbrain, pituitary fossae are partially preserved in both specimens,

356   but not sufficiently to reconstruct. The main body of the brain cavity (forebrain-hindbrain) sits

357   underneath the parietal and post-parietal bones.

358   The carotid artery canal could only be reconstructed in SNSB-BSPG 1934 VIII 514.

359   The carotid canal extends ventrally from the braincase before dividing into two canals that

360   then extend away from each other laterally. This is unlike the condition in many

361   archosauriformes where the carotid artery extends out from the pituitary fossa (Witmer *et al*.

362   2008; Witmer & Ridgely 2009; Lautenschlager & Butler 2016). This suggests the pituitary is

363   considerably reduced in *P. fergusi* and projects posteriorly. A bony margin separating the

364   pituitary from the diencephalon is not recognisable in the CT data.

365   A small ventrally positioned nerve canal reconstructed in SNSB-BSPG 1934 VII I 514

366   may be the trochlear nerve canal (iv). However, it does not sit rostrally to the trigeminal nerve

367   (v) as occurs in phytosaurs (Lautenschlager & Butler, 2016). In RC 846 and SNSB-BSPG

368   1934 VIII 514 a group of nerves were reconstructed on the lateral surface of the endocast and

369   may be the three branches of the trigeminal nerve canal (v). It seems to be in a position

370   similar to the trigeminal nerve in thalattosuchians (Brusatte *et al.* 2016; Pierce *et al.* 2016) but

371   more anteriorly positioned than in phytosaurs (Lautenschlager & Butler 2016). Similar

372   reconstructions on RC 846 μCT were considered too dorsally positioned to be cranial nerves

373   and so were identified as venous canals.

374   Anterior to the carotid artery canal on SNSB-BSPG 1934 VIII 514 is a small

375   ventrolaterally-directed nerve canal, possibly the abducens nerve (vi). This nerve is also

376   reconstructed in RC 846. In all of the reconstructions a cranial nerve sits immediately anterior

377   to the endosseous labyrinths. This nerve is similar in position to what has been interpreted as

378   the facial nerve (vii) in many extinct and extant archosauriforms (Gower & Sennikov 1996;

379   Sampson & Witmer 2007; Witmer *et al.* 2008; Witmer & Ridgely 2009; Knoll *et al.* 2012;

380   Lautenschlager *et al.* 2012; Lautenschlager *et al.* 2014; Lautenschlager & Butler 2016; Pierce

381   *et al.* 2017). The ventral portion of the braincase of RC 846 is poorly preserved, limiting the

382   reconstructions available. The endosseous labyrinths are relatively large in comparison to the

383   braincase, making up on average 7.9% the volume of the brain cavity.

384

385   *Inner Ear.* The endosseous labyrinths of all three specimens were reconstructed completely

386   (Fig. 3). The vestibular regions (top portion) of the endosseous labyrinths of *Proterosuchus*

387 *fergusi* have a pyramidal shape superficially comparable to the thalattosuchians *Steneosaurus*

388 *gracilirostris* (Brusatte *et al.* 2016) and *Pelagosuchus typus* (Pierce *et al.* 2017). While in

389 lateral view the anterior semi-circular canal (ASC) looks substantially larger than the

390 posterior semi-circular canal (PSC), the canals are actually relatively equal in their

391 proportions. This morphological feature is shared among many non-archosaurian

392 archosauriformes and early pseudosuchians (Brusatte *et al.* 2016; Lautenschlager & Butler,

393 2016; Pierce *et al.* 2016; Sobral *et al.* 2016b) but is thought to be a plesiomorphic trait lost in

394 extinct and extant crocodylomorphs, which tend to have considerably larger anterior canals

395 compared to the posterior canal (Georgi & Sipla 2008; Witmer *et al.* 2008; Witmer & Ridgely

396 2009; Pierce *et al.* 2017). The ASC and LSC are elliptical in shape, whereas the PSC is

397 straighter. The PSC of SNSB-BSPG 1934 VIII 514 has a pronounced ventrally-directed kink,

398 unlike the condition in RC 846. This feature is more pronounced in the right PSC and

399 therefore likely the result of post-mortem deformation of the specimen (Fig. 3C-D).

400   The endosseous cochlear duct (ECD) is significantly less ventrally extended than in

401 other archosauriform reconstructions (e.g. Lautenschlager & Butler 2016; Brusatte *et al.*

402 2016; Pierce *et al.* 2017; Leahey *et al.* 2015; Witmer *et al.* 2008). The fenestra vestibuli

403 (which connects the inner and middle ears) is visible in RC 846 and possibly in SNSB-BSPG

404 1934 VIII 514 and extends posterolaterally away from the labyrinth.

405

406 *Morphometric Outline Analysis*

407   *Brain Outlines.* EFA was used to compare the brain cavity endocast of *Proterosuchus*

408 *fergusi* to that of various extant and extinct archosauriforms. As the olfactory bulbs are only

409 reconstructed in RC 846, this endocast was outlined and analysed. The first three principal

410 component (PC) axes (Fig. 4 & Brown *et al.* 2019, fig. S2-3) account for 79.2% of shape

411 variation. *Proterosuchus fergusi* and the proterochampsian *Tropidosuchus romeri* (the only

412 other non-archosaurian archosauriform with an endocast sufficiently complete enough to be

413 included in the analysis; Trotteyn & Paulina-Carabajal 2016) fall well within the non-

414 phytosaur pseudosuchian morphospace in PC1 vs. PC2 (Fig. 4). Minimum spanning trees

415 show that *P. fergusi* is placed closest to *Sebecus icaeorhinus* (early–mid Eocene sebecid

416 crocodylomorph) and *Gavialis gangeticus* (gharial) in PC1 vs. PC2 (Brown *et al.* 2019, fig.

417 S4) and PC1 vs. PC3 (Brown *et al.* 2019, fig. S5), respectively. Both PC plots show clear

418 divisions between phylogenetic groups, with groups with similar ecological niches such as

419 birds and pterosaurs, and phytosaurs and crocodylomorphs, overlapping each other in

420 morphospace. PERMANOVA tests show significant differences between the endocranial

421 morphology of semi-aquatic and terrestrial taxa in the analysis (Table 1) as well as significant

422 support for the separation in morphospace of many groups within the clade Archosauriformes

423 (Table 2).

424

425 *Inner Ear Outlines.* EFA was used to test the anatomical variations between the inner ears of

426 diapsids, both with (w/) and without (w/o) the ECD. The first two PC axes account for 70.1%

427 and 72.9% of shape variation with (Fig. 5A) and without the ECD (Fig. 5B), respectively. In

428 both PC plots, RC 846 overlaps in morphospace with aquatic, semi-aquatic and terrestrial

429 taxa. RC 846 μCT similarly lies within all three morphospaces when the ECD is excluded

430 (Fig. 5B), but lies outside all morphospace when the ECD is included (Fig. 5A). Minimum

431 spanning trees (Brown *et al.* 2019, fig. S7A & S7B) show that both RC 846 and RC 846 μCT

432 lie closest to terrestrial squamates, with the exception of RC 846 μCT which comes out

433 closest to the sauropodomorph *Antarctosaurus wichmannianus* when the ECD is excluded

434 (Brown *et al.* 2019, fig. S7B).

435   Plots show substantial morphospace overlap between different ecological groupings.

436   However, PERMANOVA tests (Table 3) show significant differences between the inner ear

437   morphology of taxa from all ecologies when the ECD is included, and between aquatic taxa

438   and both terrestrial (p = 0.0013) and semi-aquatic taxa (p = 0.0282) when excluded.

439   Phylogenetic groupings are generally not very distinguishable in either iteration, but at higher

440   taxonomic ranks 'archosauromorphs' and 'outgroup taxa' (testudines, sauropterygians and

441   squamates) show a clear divergence when the ECD is included (Brown *et al*. 2019, fig. S8A)

442   compared to when the ECD is excluded (Brown *et al*. 2019, fig. S8B). PERMANOVA tests

443   (Table 4) show that when the ECD is included, basal archosauriforms (which includes solely

444   *Proterosuchus fergusi* in this iteration) are significantly different to all groups apart from

445   sauropterygians (p= 0.2562), testudines (p= 0.1189) and phytosaurs (0.0995). However, when

446   the ECD is excluded, basal archosauriforms (which includes both *P. fergusi* and *Euparkeria*

447   *capensis* in this iteration) are significantly different to fewer groups, including more derived

448   archosauriform groups: Phytosauria (p= 0.7363), non-phytosaurian pseudosuchians (p=

449   0.1340) and sauropods (p = 0.0618).

450

451   *Morphometric Landmark Analysis*

452   The PC plots (Fig. 6) demonstrate the variation in the morphology of the semi-circular canals

453   of diapsids based on landmarks. The three PC axes (Fig. 6A-C) account for 81.2%, 74.1% and

454   80.8% of shape variation across the ASC, LSC and PSC, respectively. CVA results (Table 5)

455   support significant differences between ecological groupings in most cases, with terrestrial

456   and aquatic taxa differing significantly across all semi-circular canals (p= 0.0002, ASC; p=

457   0.0050, LSC; p= 0.0051, PSC). RC 846 is recovered in morphospace occupied by terrestrial,

458   semi-aquatic and aquatic taxa in ASC and LSC, but places outside occupied morphospace in

459   the PSC plot. Whereas RC 846 μCT is displaced from all occupied morphospace in both the

460   PSC and LSC plots, but overlaps with aquatic taxa in the ASC plot (Fig. 6A). All three PC

461   plots seem to separate taxa by phylogenetic group relatively well; however, CVA results show

462   very few significant results between phylogenetic groupings (Table S2). Across all semi-

463   circular canals, basal archosauriforms (solely *P. fergusi*) are only significantly different to

464   Aves (p= 0.0231, ASC; p= 0.0208, LSC; p= 0.0211, PSC).

465

Head Posture

467   Relative to the horizontal, the average orientation of the LSC plane is 17.19° (Fig. 7A),

468   suggesting *Proterosuchus fergusi* had a significantly upright 'alert' head posture (Fig. 7B).

469   This is in contrast to *Crocodylus johnstoni* (freshwater crocodile), which has a horizontal head

470   posture when the LSC plane is aligned to the horizon (Fig. 7C; Witmer *et al.* 2008).

471

Auditory Abilities

473   Both the linear and PGLS regression (Fig. 8; solid line and dashed line, respectively) support

474   significant relationships between ECD length and both mean hearing and hearing range in

475   extant taxa (Fig. 8). On the basis of these relationships, the auditory abilities of *Proterosuchus*

476   *fergusi* have been estimated. Both regression lines reveal considerably different

477   reconstructions, with the linear regression predicting a mean hearing frequency of ~525Hz

478   and a hearing range of ~780Hz (similar to that of *Alligator mississippiensis* and the

479   rhynchocephalian *Sphenodon punctatus*), and the PGLS regression predicting a mean hearing

480   frequency of ~1275Hz and a hearing range of ~2150Hz (similar to that of the terrestrial

481   squamate *Ptyodactylus hasselquistii*).

482

483   *Snout Beam Analysis*

484   Plots generally show similar trends in all taxa, with second moment and moment of inertia

485   values generally increasing steadily posteriorly along the rostra (Fig. 9). Pertaining to the

486   anterior 20% of the rostrum of *Proterosuchus fergusi*, differences between the straight and

487   curved beam (Fig. 9, solid and dashed line, respectively) analysis are relatively consistent

488   across all plots; with the straight beam showing a more posteriorly positioned peak (~15%

489   along the rostrum length) compared to the curved beam (~4% along the rostrum length).

490   *Tomistoma schlegelii* (false gharial) is the only comparative taxa that is significantly different

491   to *P. fergusi* across all iterations of the analysis and all moments of resistance (Table S4).

492   Values of Ix, which represents resistance to dorsoventral bending, (Fig. 9A-B) are highest in

493   *Proterosuchus fergusi*, even when other taxa are size-corrected. True size plots show that

494   *Atractosteus spatula* (alligator gar) is the least resistant (Fig. 9A), but when scaled *Tomistoma*

495   *schlegelii* is the least (Fig. 9B). Paired t-test results from the straight beam iteration show that

496   there is no significant difference in resistance along the whole rostrum between *P. fergusi* and

497   the crocodylids when scaled (Table S4), but it is worth noting that this is not the case when a

498   curved beam is used instead.

499   Resistance to mediolateral bending (Iy) is very similar between *Proterosuchus fergusi*

500   and the crocodylids when scaled (Fig. 9C) This is also demonstrated by the paired t-test

501   results, which show no significant differences in Iy values between *P. fergusi* and the

502   crocodylids at true size (Table S4). However, when taxa are size-corrected *P. fergusi* has

503   relatively poor resistance compared to the other taxa (Fig. 9D).

504   Resistance to torsion (J) is the sum of Ix and Iy and so follows the general trends of Ix

505   and Iy. *Proterosuchus fergusi* has J values very similar to *Crocodylus rhombifer* and

506   *Crocodylus moreletii* at true size (Fig. 9E; Table S4). When taxa are scaled, all species have

507   very similar torsion resistance, except *T. schlegelii* which is much lower (Fig. 9F).

508

509   **DISCUSSION**

510

511   *Life habits of* Proterosuchus

512   *Hearing.* The lower portion of the inner ear contains the ECD, which comprises sound-

513   detecting cells that are stimulated by sound waves transmitted from the middle ear (Sobral *et*

514   *al.* 2016b). The virtual reconstruction of the ECD of *Proterosuchus fergusi* has permitted an

515   estimation of the mean hearing frequency (MHF) and hearing range (HR). In order to

516   understand the effects that phylogeny has on these interpretations, a PGLS regression was

517   also used in addition to the linear regression proposed by Walsh *et al.* (2009). The regressions

518   gave different results, with sensitivity range estimations of ~0.1–0.9 kHz and ~0.2–2.4 kHz

519   for the linear and PGLS regressions, respectively. However, despite differences, results from

520   both iterations concur that *P. fergusi* was probably more specialised to lower frequencies,

521   much like modern crocodiles (Vergne *et al.* 2009; Walsh *et al.* 2009). Following the results of

522   the linear regression, acoustic estimations for *P. fergusi* are on the lower end of sensitivity

523   values known for modern crocodylians (Walsh *et al.* 2009), as well as the extinct

524   crocodyliforms such as the thalattosuchian *Steneosaurus cf. gracilirostris* (Brusatte *et al.*

525   2015) and the basal euschian *Lohuecosuchus megadontos* (Serrano-Martínez *et al.* 2019), for

526   which auditory acuity has also been estimated.

527   Estimations of auditory ability can also be informative in understanding the vocal

528   complexity of a species. Considered to have resulted from coevolution of the vocal and

529   auditory systems, individuals can typically only perceive frequencies within their own vocal

530   range (Narins *et al.* 2004). Vocality of a species can be used to infer behavioural aspects such

531   as social complexity and ecology (Walsh *et al.* 2009; Walsh *et al.* 2014).

532   Sociality and vocality are integrally linked, with research suggesting social complexity

533   has driven both vocal complexity and cognition in vertebrates (Blumstein & Armitage 1997;

534   Freeberg *et al.* 2012; Freeberg & Krams 2015; Sewall 2015). Species that form larger and

535   more complex social systems require a more complex vocal system to work together

536   effectively. Therefore, vocal range, and thus auditory range, can be indicative of group size in

537   a species. This is supported by results from Walsh *et al.* (2009) which found significant

538   correlations between increased ECD length and larger social aggregations. Following this, the

539   small ECD reconstructed in *P. fergusi* could suggest that it lived in small groups, or was even

540   solitary.

541   In closed environments where visual communication is less effective (such as dense

542   jungles), vocal and auditory complexity is highly advantageous (Garrick & Lang 1977;

543   Brown & Waser 1984). In this study we find the relatively low acoustic complexity

544   interpreted for *P. fergusi* to be consistent with the proposed absence of forests and vegetation

545   following the Permo-Triassic mass extinction in the Karoo (Smith 1995; Ward *et al.* 2000;

546   Smith *et al.* 2012). However, it is worth noting that while vocalisation and hearing ability in

547   mammals is thought to be suggestive of habitat type (Brown & Waser 1984; de la Torre &

548   Snowdon 2002), within living archosaur groups the relationship remains ambiguous (Garrick

549   & Lang 1977; Nicholls & Goldizen 2006; Mason & Burns 2015).

550

551   *Olfaction.* The recognition of olfactory cues (sense of smell) is important for interspecific

552   communication (e.g. kin recognition, finding a mate, territorial markers), navigation (e.g.

553   foraging, predation, finding shelter and other resources), and avoiding dangers (e.g. predator

554   identification, poisonous food) (Dial & Schwenk 1996; Hemila & Reuter 2008; Krause *et al.*

555   2012; Müller *et al.* 2018). The olfactory bulbs, located anterior to the forebrain, contain

556   olfactory receptor (OR) proteins that are responsible for detecting odorants (Freitag *et al.*

557   1998). The size of the olfactory bulbs generally corresponds to the quantity of OR proteins

558   (Steiger *et al.* 2009), meaning that the enlargement of the olfactory bulbs is often indicative of

559   increased olfactory abilities. Following this, the size of the olfactory bulbs has been widely

560   used as a proxy for olfactory acuity in fossil taxa (Benton 1983; Brochu 2000; Kundrát 2007;

561   Witmer *et al.* 2008; Witmer & Ridgely 2009; Zelenitsky *et al.* 2009; Bourke *et al.* 2014; Sales

562   & Schultz 2014). The presence of olfactory fossae along the ventral surface of the frontals has

563   allowed for the reconstruction of the olfactory bulbs in *Proterosuchus fergusi* (Fig. 2). The

564   olfactory bulbs are analogous in relative size and shape to many modern crocodylians (Pritz

565   1975; Witmer *et al.* 2008; Jirak & Janacek 2017). Many crocodylians are considered to have a

566   well-developed sense of smell, capable of quickly locating carrion both in the water and on

567   land (Weldon *et al.* 1990). This suggests that proterosuchids may have had a similar olfactory

568   acuity to modern crocodiles.

569   A latex endocast of *Tasmaniosaurus triassicus*, a sister-taxon to Archosauriformes

570   (Ezcurra 2016) (previously considered a proterosuchid (Camp & Banks 1978)), revealed

571   olfactory bulbs that were 1.4 times wider than the maximum width of the cerebrum (Ezcurra

572   2014). In *P. fergusi* the olfactory bulbs are only ~60% the maximum width of the cerebrum,

573   suggesting significant differences in the life habits of these two Early Triassic carnivores.

574   Ezcurra (2014) suggested the large olfactory bulbs in *T. triassicus* were indicative of a

575   terrestrial ecology, following a study showing larger olfactory bulbs in fully terrestrial

576   carnivorans in comparison to those with an aquatic affinity (Gittleman 1991). While the

577   relationship between olfaction and habitat is more ambiguous in reptiles than mammals

578   (Marek *et al.* 2015; Müller *et al.* 2018), the striking difference in relative olfactory width in

579   these two phylogenetically similar taxa suggests that *P. fergusi* may have been more adapted

580   to aquatic environments than *T. triassicus*.

581

582   *Prey Choice.* Historically proterosuchids were considered aquatically-based predators,

583   feeding on fish (Tatarinov 1961) and tetrapods, such as the dicynodont therapsid *Lystrosaurus*

584   (Reig 1970). *Proterosuchus fergusi* occurs between 5–14 metres above the Permo-Triassic

585   boundary in the lower levels of the *Lystrosaurus* AZ of the Karoo Basin (Smith & Botha-

586   Brink 2014). During the deposition of these rocks there was a high abundance of potential

587   prey items for *P. fergusi*, including dicynodont (e.g. *Lystrosaurus* spp.) and therocephalian

588   (e.g. *Moschorhinus* and *Promoschorhynchus*) synapsids (Smith & Botha-Brink 2014).

589   However, as no direct evidence of proterosuchid diet has been found (i.e. preserved gut

590   contents), only indirect evidence such as tooth morphology and general anatomy can be used

591   to infer feeding habit (Ezcurra *et al.* 2013).

592   Results of the rostral beam analysis show that the more oreinirostral morphology of *P.*

593   *fergusi* was highly resistant to bending forces and torsion, comparable to the typically

594   platyrostral morphology in *Crocodylus rhombifer* and *Crocodylus moreletii* (Fig. 9, Table

595   S4). These results are consistent with finite element analyses from Rayfield & Milner (2008)

596   comparing oreinirostral and platyrostral morphologies. The two *Crocodylus* species included

597   in this analysis are generalists, feeding on a variety of prey items, including fish, amphibians,

598   reptiles, birds and mammals (Platt *et al.* 2006; Milián-García *et al.* 2011). Juvenile and

599   subadult crocodiles have an even more varied diet, with large quantities of invertebrates,

600   gastropods and small vertebrates (Platt *et al.* 2006). Similarly, in *P. fergusi* the more gracile

601   skull and relatively longer teeth of juvenile specimens has been thought to suggest that

602   different ontogenetic stages favoured different prey items, possibly to decrease intraspecific

603   competition (Ezcurra & Butler 2015b). *Proterosuchus fergusi* may have had a generalist diet

604   like modern crocodylians that change their diet through ontogeny from largely invertebrates

605   to large terrestrial vertebrates. *Proterosuchus fergusi* and the platyrostral crocodylians

606   (*Alligator mississippiensis*, *C. rhombifer*, *C. moreletii*) show significant differences in

607   bending resistance to the longirostrine false gharial (*Tomistoma schlegelii*) in the analyses

608   (Fig. 9, Table S4). This difference reflects the more specialist life habit of *T. schlegelii* with a

609   predominately piscivorous diet (Pierce *et al.* 2008).

610

611   *Ecological adaptations.* Despite the presence of eleven well preserved specimens of

612   *Proterosuchus fergusi*, there is currently no consensus on their ecology, or on the ecology of

613   proterosuchids as a whole (Ezcurra *et al.* 2013). Original interpretations of a semi-aquatic

614   habit for *P. fergusi* were in part due to the supposedly wet climate and palustrine

615   environments presumed of the *Lystrosaurus* AZ. However, recent studies have shown that the

616   Karoo Basin at this time was drastically different. Sedimentological analyses show the region

617   was predominately semi-arid with vast braided rivers resulting from lack of vegetation (Smith

618   1995; Ward *et al.* 2000; Smith *et al.* 2012) and the climate fluctuated between droughts,

619   sporadic flood events and extreme cold snaps (Smith 1995; Smith & Ward 2001; Viglietti *et*

620   *al.* 2013; Smith & Botha-Brink 2014).

621   Endocranial reconstructions of the two *P. fergusi* specimens have not allowed us to

622   make sound interpretations of its ecology based on palaeoneurology. Statistical tests of the

623   brain cavity outline morphology (Table 1) show significant differences only between

624   terrestrial and semi-aquatic taxa. This difference however is likely explained by the

625   evolutionary divergence between predominately terrestrial avemetatarsalians and

626   predominately semi-aquatic pseudosuchians. Similar morphometric analyses on the

627   endosseous labyrinth of saurians (Fig. 5) better separate groups based on ecology (Table 3),

628   but also seem to be highly constrained by phylogeny (Table 4). The landmark-based analysis

629   on individual semi-circular canals (Fig. 6) appears to be more appropriate for looking at

630   ecology; statistical analyses show significant differences between the majority of ecological

631   groupings (Table 5) and comparatively poor separation of phylogenetic groupings (Table S2).

632   Across all three canals, *P. fergusi* resides consistently close to predominately semi-aquatic

633   and aquatic taxa from various phylogenetically-distant groups (particularly sauropterygians,

634   squamates and pseudosuchians). While the relationships between ecology, locomotion and

635   function of a taxon and the endocranial anatomy are currently uncertain, several studies have

636   recently attempted to elucidate this by looking at the morphology of the endosseous labyrinths

637   (Cuthbertson *et al.* 2015; Yi & Norell 2015; Benson *et al.* 2017; Neenan *et al.* 2017). Based

638   on our results, the endosseous labyrinths seem to be most appropriate for this type of analysis,

639   particularly when individual semi-circular canals are separately analysed. If morphological

640   differences are found to be indicative of ecological variation, with endosseous labyrinths

641   comparable to various amphibious taxa, it is reasonable to postulate that *P. fergusi* may have

642   had the sensory and balance organs required for semi-aquatic life.

643   In life, the endosseous labyrinths (semi-circular canals) are part of the vestibular

644   system, responsible for balance and co-ordination. Endolymph fluid moves back and forth

645   through each of the canals as the skull rotates, triggering receptors at the end of the canals that

646   send signals to the brain (Clack 2016). Unlike the auditory organs, the function of these

647   vestibular organs has largely remained constant over vertebrate evolution (Carey & Amin

648   2006) allowing extant animals to be used as analogues to inform about the balance of early

649   tetrapods. For nearly a century many tetrapods have been thought to habitually hold the lateral

650   semi-circular canal (LSC, or sometimes 'horizontal semi-circular canal') horizontally

651   (Lebedkin 1924; de Beer 1947; Duijm 1951). Following this, over the last two decades the

652 LSC has been widely used to infer the head posture (typically 'alert' or 'resting') of various

653 fossil groups (Rogers 1998; Witmer *et al.* 2003; Sampson & Witmer 2007; Sereno *et al.* 2007;

654 Witmer *et al.* 2008; Witmer & Ridgely 2009; Neenan & Scheyer 2012; Benoit *et al.* 2017).

655 The average orientation of the LSC in *P. fergusi* specimens SNSB-BSPG 1934 VIII 514 and

656 RC 846 reconstructed in this study was ~17° (Fig. 7A), suggesting *P. fergusi* held its head

657 tilted upwards (Fig. 7B). Among the array of taxa for which head posture has been inferred in

658 this way, up tilted expressions are generally uncommon, especially to the degree found in *P.*

659 *fergusi* (Marugán-Lobón *et al.* 2013). While the use of the LSC in inferring head posture has

660 been met with scepticism, due to variation of inferred head postures found within

661 phylogenetically similar groups (Hullar 2006; Taylor *et al.* 2009; Marugán-Lobón *et al.*

662 2013), several studies have suggested a possible relationship between the LSC and the

663 resulting head posture linked to ecological factors (e.g. diet, feeding behaviour) and supported

664 by osteological correlates (i.e. occipital position) (Sereno *et al.* 2007; Neenan & Scheyer

665 2012; Schellhorn 2018). If LSC orientation does show a behavioural and/or ecological signal,

666 the range of LSC orientations recorded in the two specimens of *P. fergusi* indicate an

667 upturned head posture and could be interpreted as an adaption to semi-aquatic life. When

668 upturned ~17° the bones of the cranial roof lie almost horizontally and the vertically

669 positioned external nares are about level with orbit height. When in the water, *P. fergusi*

670 would be able to keep its eyes and nostrils out of the water while keeping a low profile close

671 to the waterline with the rest of its body remaining fully submerged, alike to modern day

672 crocodiles. As previously discussed, dorsally-positioned external nares are an adaptation to

673 aquatic and semi-aquatic life that has convergently evolved in numerous groups over

674 vertebrate evolution. Perhaps the upturned head posture of *P. fergusi* represents an alternative

675 secondary adaptation for a semi-aquatic lifestyle among early diapsids. This would concur

676 with the upwards tilting skull of *Lystrosaurus* (Benoit *et al.* 2017), which were

677   contemporaneous to proterosuchids and have likewise also been interpreted as possibly semi-

678   aquatic (Retallack *et al.* 2003; Ray *et al.* 2005).

679

680   *Functional morphology of the premaxilla*

681   The overhanging premaxilla that characterises proterosuchids is enigmatic in origin and

682   function. While unique in its accentuation, the snout morphology is analogous with several

683   extant and extinct vertebrate groups. Within the clade Archosauriformes, ornithosuchids such

684   as *Riojasuchus* and *Ornithosuchus* exhibit a superficially similar snout morphology to

685   *Proterosuchus*. However, the comparatively few specimens known for ornithosuchids mean

686   that limited information can be obtained about the functional morphology and evolution of

687   this trait within archosauriforms. Modern analogues allow for the study of functional and

688   sexual dimorphic aspects of this bizarre snout morphology. While phylogenetically distant,

689   actinopterygians including *Oncorhynchus kisutch* (coho salmon) (Ezcurra 2017) and (to a

690   lesser extent) many lepisosteids (gar) have a downturned premaxilla that does not fully

691   occlude with the lower jaw. In *O. kisutch*, this trait is sexually selected for and found only in

692   the hooknose adult male morphotype of the species (Fleming & Gross 1994). By contrast, in

693   lepisosteids, this trait is thought to be functional in predation, for manipulating prey following

694   capture (Lauder & Norton 1980).

695   Convergent features in fossil and living taxa have long been interpreted as inferring shared

696   function, even between highly phylogenetically-distant groups (e.g. Ji *et al.* 2006; Field *et al.*

697   2011; O'Brien *et al.* 2016; Vullo *et al.* 2016; Arbour & Zanno 2019). Vullo *et al.* 2016

698   commented on the morphological similarities between the jaws of spinosaurid dinosaurs and

699   an extant group of anguilliform fish (pike conger eels) and suggested that this inferred shared

700   feeding behaviours. The lepisosteid *Atractosteus spatula* (alligator gar) was among

701 comparative taxa analysed for rostral resistance because of its overhanging premaxilla. Albeit

702 far less accentuated compared to *Proterosuchus fergusi,* comparing results between the two

703 overhanging premaxillae may have identified signals unique to this trait. The various

704 statistical analyses tend to show significant differences between *P. fergusi* and *A. spatula*

705 (Table S4). These results may suggest that *P. fergusi* did not share a similar method of

706 predation to lepisosteids.

707   Growing and maintaining an oversized premaxilla with up to 18 ankylothecodont

708 (deeply rooted and fused to the bone) teeth that would undergo periodic replacement, made

709 the snout a costly phenotype (Ezcurra 2017). As such, without a morphological function, this

710 trait would likely been negatively selected out of the population by natural selection

711 (Andersson 1994). To date no physiological function has been suggested and mechanical

712 functions such as digging have been ruled out after macroscopic analysis on the premaxillary

713 teeth (Ezcurra 2017). The ontogenetic changes in the snout morphology (Ezcurra & Butler

714 2015b) and phenotypic costliness led Ezcurra (2017) to propose social and sexual selection as

715 a possible explanation.

716   Snout beam analyses suggest that the premaxilla of *P. fergusi* is considerably resistant

717 to dorsoventral bending and torsion compared to the crocodylians (Fig. 9; Table S4). The

718 overhanging premaxilla does not seem to enhance or reduce resistance to mediolateral

719 bending. The high resistance of the premaxilla to dorsoventral bending may be an indication

720 of a specialist predation method. If this specialist function was beneficial enough it would

721 outweigh the costliness of the premaxilla. However advanced biomechanical analyses such as

722 finite element analysis would be required to test this hypothesis. It is possible that this

723 phenotype may have been positively selected for under sexual selection, with a larger

724 overhanging premaxilla being a signal for increased physical strength. While presumably

725 sexual dimorphism was as widespread among fossil saurians as it is today, recognising sexual

726 dimorphism and even distinguishing gender is extremely difficult and problematic in the

727 saurian fossil record (Bonnan *et al.* 2008; Ezcurra 2017; Mallon 2017). One aspect of sexual

728 selection that could possibly be ruled out is the 'handicap principle' proposed by Zahavi

729 (1975). The handicap principle states that survival of an individual to sexual maturity with a

730 'handicap' (in this instance the costly overhanging premaxilla) is evidence of overall fitness

731 and therefore a suitable mate (Zahavi 1975; 1977). Resistance tests show that the premaxilla

732 is not detrimental to rostral strength, therefore it is likely not a 'handicap' and this might not

733 be a viable explanation of the phenotype.

734

735 *Implications for the evolution of Archosauriformes*

736 *Evolution of the archosauriform brain.* The endocasts of *Proterosuchus fergusi* reconstructed

737 in this study are important contributions to understanding the evolution of basal

738 archosauriform neuroanatomy (Fig. 10). While the palaeoneurology of archosaurian clades

739 (particularly Dinosauria) have been extensively studied, stem archosaurs have been widely

740 overlooked. Prior to this study, the endocranial anatomy of only three specimens of non-

741 archosaurian archosauriform had been virtually reconstructed (Trotteyn & Paulina-Carabajal

742 2016; Fabbri *et al.* 2017) to add to the small number of informative artificial endocasts

743 (Benton 1983; Gower & Sennikov 1996; Wharton 2000). Trotteyn & Paulina-Carabajal

744 (2016) reconstructed the endocranium of the proterochampsian *Tropidosuchus romeri,* while

745 Fabbri *et al.* (2017) reconstructed the endocranium of *P. fergusi* (RC 846 – although Fabbri *et*

746 *al.* incorrectly identified the specimen as 'RC 96' which actually corresponds to a dicynodont

747 (Ezcurra 2015)) and *E. capensis*. However, the endocasts from Fabbri *et al.* (2017) are

748 incompletely figured and not described in the text and are therefore largely uninformative in

749 regard to the morphology of the early archosauriform brain cavity.

750   Results of the morphometric analysis show that convergence in brain morphology has

751 occurred multiple times in the archosauriform lineage, particularly in groups with similar life

752 habits. A clear example of this is the significant overlap between bird and pterosaur brain

753 morphology, both of which share a volant mode of life. These analyses also highlight

754 similarities between the brain cavities of pseudosuchians and basal archosauriforms,

755 especially when compared to avemetatarsalians. In some archosauriform groups (particularly

756 non-avian theropods and avialans), endocranial morphology has been tentatively linked to

757 orbit size, locomotion, ecology and organisation of cranial elements (Bhullar *et al.* 2012;

758 Kawabe *et al.* 2013; Balanoff & Bever 2017; Fabbri *et al.* 2017). Perhaps with further

759 research the correlations between form and function of the endocranial anatomy will become

760 better understood and explain some of the similarities between relatively phylogenetically-

761 distant taxa that our study displays.

762

763 *Evolution of the archosauriform inner ear.* The functional morphology and early evolution of

764 the endosseous labyrinth is important for understanding the rise of archosaurs in the

765 Mesozoic. Prior to this study no non-archosaurian archosauriform inner ear had been

766 completely reconstructed (Fig. 11), leaving a significant gap in our understanding of how the

767 vestibular and auditory systems have evolved in stem archosaurs.

768   In many eusuchians, the ASC is significantly longer compared to the PSC (Georgi &

769 Sipla 2008; Witmer *et al.* 2008; Brusatte *et al.* 2016; Pierce *et al.* 2017). However, in more

770 basal archosauriforms, the ASC and PSC are much more equal in size (Kley *et al.* 2010;

771 Brusatte *et al.* 2016; Lautenschlager & Butler 2016; Sobral *et al.* 2016b; Pierce *et al.* 2017).

772 Pierce *et al.* (2017) proposed that more equally proportioned anterior and posterior canals are

773 plesiomorphic for Archosauriformes. The relatively equal size of the ASC and PSC in the

774　endosseous labyrinths reconstructed for *P. fergusi* is consistent with these interpretations. The

775　relatively equal size of the ASC and PSC in phytosaurs has been suggested to be indicative of

776　limited neck movement and semi-aquatic habitat (Sobral & Müller 2017). However, this

777　seems unlikely as extant crocodiles inhabit semi-aquatic ecosystems and have relatively

778　limited neck movements. Further research is required to determine the functionality of this

779　derived trait in eusuchians.

780　　　　The inner ears of archosaurs are significantly different to those of other diapsid

781　groups. One of the most striking differences is the comparatively long ECD possessed by both

782　crocodile-line and bird-line archosaurs. This trait seems to be confined to archosaurs, with

783　most diapsid groups outside of Archosauromorpha (e.g. squamates, rhynchocephalians,

784　testudines and sauropterygians) having relatively short cochlear ducts. Pierce *et al.* (2017)

785　suggested that within Pseudosuchia the elongated cochlear duct evolved crownward to

786　phytosaurs due to the small ECD present in the phytosaurs *Ebrachosuchus* and *Parasuchus*

787　reconstructed by Lautenschlager & Butler (2016). However, Lautenschlager & Butler (2016)

788　stated that the two phytosaur specimens were dorsoventrally compressed by ~40% and so the

789　raw endocasts are not representative of true scale. When retrodeformed (Fig. 11E-F) the

790　cochlear ducts are superficially and morphometrically similar to other pseudosuchians (Fig.

791　5A). Following this, the presence of the derived cochlear trait in both crocodile-line and bird-

792　line archosaurs suggests the evolution of the trait occurred before Avemetatarsalia and

793　Pseudosuchia diverged. However, prior to this study, the lack of labyrinth reconstructions in

794　stem archosaurs meant that the origin of this trait could not be further constrained.

795　　　　Reconstructions of the endosseous labyrinth reveal *P. fergusi* to have a relatively

796　small ECD compared to crown archosaurs (Fig. 2; Fig. 11B). Morphometric analyses of the

797　inner ear place *P. fergusi* close to non-archosaurian diapsids when the ECD is included,

798　suggesting that the small ECD is a plesiomorphic trait (Fig. 5A). Following this it could be

799   postulated that the elongated ECD first evolved in archosauromorphs crownward of *P.*

800   *fergusi*. As *P. fergusi* is the most basal member of the clade Archosauriformes (Nesbitt 2011),

801   the most parsimonious inference is that a small cochlear duct is a plesiomorphic trait found in

802   basal diapsids and retained in lepidosauromorphs and basal archosauromorphs. Subsequently,

803   the derived trait of an elongate duct evolved somewhere in stem archosaurs and was retained

804   in both avemetatarsalians and pseudosuchians. As a ventrally-extended ECD has been linked

805   to increased auditory acuity (as previously discussed), perhaps the evolution of this derived

806   trait marked a significant increase in auditory ability, vocality, sociality and cognition, all of

807   which are thought to be integrally linked (Blumstein & Armitage 1997; Freeberg *et al.* 2012;

808   Freeberg & Krams 2015; Sewall 2015). These developments may potentially have contributed

809   to the radiation of archosaurs during the Triassic and Early Jurassic.

810

CONCLUSIONS

812   This study presents the first in-depth assessment of the braincase and inner ear of the Early

813   Triassic basal archosauriform *Proterosuchus fergusi*. Morphological comparisons of

814   endocranial reconstructions, supplemented by analyses on the skull posture, rigidity and

815   auditory abilities, have revealed much about the probable life habits of *P. fergusi* and the

816   evolution of the brain and inner ear through early archosauriform evolution. Endocranial

817   reconstructions reveal *P. fergusi* had: (1) an endocranial cavity with low-angle brain flexures;

818   (2) medium-sized olfactory bulbs; (3) pyramidal and sub-equally-sized semi-circular canals;

819   (4) a small cochlear duct.

820   The brain morphology of *P. fergusi* is superficially and statistically similar to modern

821   crocodylians and phytosaurs, and different to birds, pterosaurs and non-avian theropods.

822   Assessment of the endocranial anatomy suggests that *P. fergusi* is estimated to be specialised

823   to lower frequency sounds, with a proficient sense of smell, both comparable to modern

824   crocodiles. *Proterosuchus fergusi* held its head upwards ~17°, perhaps representing an

825   alternative adaptation to semi-aquatic life than dorsally-positioned nares and orbits. The

826   overhanging premaxilla remains largely enigmatic; with beam theory analyses indicating that

827   generally this unusual morphology neither strengthens or weakens the snout and therefore

828   purely non-functional selection pressures for this trait may be ruled out.

829   The small ECD of *P. fergusi* suggests basal archosauromorphs retained an ancestrally

830   small ECD which later evolved to become elongate in more derived archosauriforms, before

831   the divergence of avemetarsalians and pseudosuchians. The increase in auditory complexity

832   as a result of an elongated ECD may indicate the coevolution of increased cognitive abilities,

833   vocality and sociality in stem archosaurs, which could in turn have contributed to the

834   radiation of archosaurs in the Triassic, forging the way for dinosaurs to dominate global

835   faunas during the Mesozoic.

836

842

REFERENCES

845   ALLEMAND, R., BOISTEL, R., DAGHFOUS, G., BLANCHET, Z., CORNETTE, R.,
846   BARDET, N., VINCENT, P. and HOUSSAVE, A. 2017. Comparative morphology of
847   snake (Squamata) endocasts: evidence of phylogenetic and ecological signals. *Journal of*
848   *Anatomy*, **231**, 849–868.

849   ANDERSSON, M. 1994. *Sexual Selection*, Princeton University Press, 624 pp.

850   ARBOUR, V. M. and ZANNO, L. E. 2019. Tail Weaponry in Ankylosaurs and Glyptodonts:
851   An Example of a Rare but Strongly Convergent Phenotype. *The Anatomical Record*.
852   doi.org/10.1002/ar.24093

853   BACZKO, M. B. VON and DESOJO, J. B. 2016. Cranial anatomy and palaeoneurology of
854   the archosaur *Riojasuchus tenuisceps* from the Los Colorados Formation, La Rioja,
855   Argentina. *PLoS ONE*, **11,** e0148575.

856   BALANOFF, A. M., BEVER, G. S., COLBERT, M. W., CLARKE, J. A., FIELD, D. J.,
857   GIGNAC, P. M., KSEPKA, D. T., RIDGELY, R. C., SMITH, N. A., TORRES, C. R. and
858   WALSH, S. 2016. Best practices for digitally constructing endocranial casts: examples
859   from birds and their dinosaurian relatives. *Journal of Anatomy*, **229**, 173–190.

860   BALANOFF, A. M. and BEVER, G. S. 2017. The Role of Endocasts in the Study of Brain
861   Evolution. 223-241. *In* KAAS, J. (ed.). *Evolution of Nervous Systems (2nd edition)*.
862   Academic Press, 2007 pp.

863   BENOIT, J., MANGER, P. R., FERNANDEZ, V. and RUBIDGE, B. S. 2017. The bony
864   labyrinth of late Permian Biarmosuchia: palaeobiology and diversity in non-mammalian
865   Therapsida. *Palaeontologia africana*, **52**, 58–77.

866   BENSON, R. B., STARMER-JONES, E., CLOSE, R. A. and WALSH, S. A. 2017.
867   Comparative analysis of vestibular ecomorphology in birds. *Journal of Anatomy*, **231**,
868   990-1018.

869   BENTON, M. J. 1983. The Triassic reptile *Hyperodapedon* from Elgin: functional
870   morphology and relationships. *Philosophical Transactions of the Royal Society of London.*
871   *Series B, Biological Sciences*, **302**, 605–718.

872   BENTON, M. J. and TWITCHETT, R. J. 2003. How to kill (almost) all life: the end-Permian
873   extinction event. *Trends in Ecology & Evolution*, **18**, 358–365.

874   BHULLAR, B. A. S., MARUGÁN-LOBÓN, J., RACIMO, F., BEVER, G. S., ROWE, T. B.,
875   NORELL, M. A. and ABZHANOV, A. 2012. Birds have paedomorphic dinosaur skulls.
876   *Nature*, **487**, 223.

877   BLUMSTEIN, D. T. and ARMITAGE, K. B. 1997. Does sociality drive the evolution of
878   communicative complexity? A comparative test with ground-dwelling sciurid alarm calls.
879   *The American Naturalist*, **150**, 179–200.

880   BONHOMME, V., PRASAD, S. and GAUCHEREL, C. 2013. Intraspecific variability of
881   pollen morphology as revealed by elliptic Fourier analysis. *Plant Systematics and*
882   *Evolution*, **299**, 811–816.

883   BONKE, R., WHITAKER, N., ROEDDER, D. and BOEHME, W. 2015. Vocalizations in two
884   rare crocodilian species: A comparative analysis of distress calls of *Tomistoma schlegelii*
885   (Müller, 1838) and *Gavialis gangeticus* (Gmelin, 1789). *North-Western Journal of*
886   *Zoology*, **11**, 151–162.

887   BONNAN, M. F., FARLOW, J. O. and MASTERS, S. L. 2008. Using linear and geometric
888   morphometrics to detect intraspecific variability and sexual dimorphism in femoral shape

889   in *Alligator mississippiensis* and its implications for sexing fossil archosaurs. *Journal of*
890   *Vertebrate Paleontology*, **28**, 422–431.

891   BOTHA-BRINK, J. and SMITH, R. M. 2011. Osteohistology of the Triassic
892   archosauromorphs *Prolacerta*, *Proterosuchus*, *Euparkeria*, and *Erythrosuchus* from the
893   Karoo Basin of South Africa. *Journal of Vertebrate Paleontology*, **31**, 1238–1254.

894   BOURKE, J. M., RUGER PORTER, W. M., RIDGELY, R. C., LYSON, T. R.,
895   SCHACHNER, E. R., BELL, P. R. and WITMER, L. M. 2014. Breathing life into
896   dinosaurs: tackling challenges of soft-tissue restoration and nasal airflow in extinct
897   species. *The Anatomical Record*, **297**, 2148–2186.

898   BROCHU, C. A. 2000. A digitally-rendered endocast for *Tyrannosaurus rex*. *Journal of*
899   *Vertebrate Paleontology*, **20**, 1–6.

900   BROILI, F. and SCHRÖDER, J. 1934. Beobachtungen an Wirbeltieren der Karroo
901   Formation. V. Über *Chasmatosaurus vanhoepeni* Haughton. *Sitzungsberichte der*
902   *Bayerischen Akademie der Wissenschaften, Mathematisch-Naturwissenschaftliche*
903   *Abteilung*, **3**, 225–264.

904   BROOM, R. 1903. On a new reptile (*Proterosuchus fergusi*) from the Karroo beds of
905   Tarkastad, South Africa. *Annals of the South African Museum*, **4**, 159–164.

906   BROWN, C. H. and WASER, P. M. 1984. Hearing and communication in blue monkeys
907   (*Cercopithecus mitis*). *Animal Behaviour*, **32**, 66–75.

908   BROWN, E. E., BUTLER, R. J., EZCURRA, M. D., BHULLAR, A.-B. and
909   LAUTENSCHLAGER, S. 2019. Endocranial anatomy and life habits of the Early Triassic
910   archosauriform *Proterosuchus fergusi*. *Dryad Digital Repository*.
911   https://datadryad.org/review?doi=doi:10.5061/dryad.XXXX

912   BRUSATTE, S. L., MUIR, A., YOUNG, M. T., WALSH, S., STEEL, L. and WITMER, L.
913   M. 2016. The braincase and neurosensory anatomy of an Early Jurassic marine
914   crocodylomorph: implications for crocodylian sinus evolution and sensory transitions. *The*
915   *Anatomical Record*, **299**, 1511–1530.

916   BUTTON, D. J., LLOYD, G. T., EZCURRA, M. D. and BUTLER, R. J. 2017. Mass
917   extinctions drove increased global faunal cosmopolitanism on the supercontinent Pangaea.
918   *Nature Communications*, **8**, 733.

919   CAMP, C. L. and BANKS, M. R. 1978. A proterosuchian reptile from the Early Triassic of
920   Tasmania. *Alcheringa*, **2**, 143–158.

921   CAREY, J. and AMIN, N. 2006. Evolutionary changes in the cochlea and labyrinth: solving
922   the problem of sound transmission to the balance organs of the inner ear. *The Anatomical*
923   *Record*, **288**, 482–490.

924   CHEN, Z. Q. and BENTON, M. J. 2012. The timing and pattern of biotic recovery following
925   the end-Permian mass extinction. *Nature Geoscience*, **5**, 375–383.

926   CLACK, J. A. 2016. Vertebrate diversity in a sensory system: the fossil record of otic
927   evolution. 1–16. *In* CLACK, J. A., FAY, R. R., POPPER, A. N. (eds). *Evolution of the*
928   *vertebrate ear*. Springer, 355 pp.

929   CORFIELD, J. R., KUBKE, M. F. and KÖPPL, C. 2013. Emu and kiwi: the ear and hearing
930   in Paleognathous birds. 263–287. *In* KÖPPL, C., MANLEY, G. A., POPPER, A. N. and
931   FAY, R. R. (eds). *Insights from comparative hearing research.* Springer, 388 pp.

932   CRAMPTON, J.S. 1995. Elliptic Fourier shape analysis of fossil bivalves: some practical
933   considerations. *Lethaia*, **28**, 179–186.

934   CRUICKSHANK, A. R. I. 1972. The proterosuchian thecodonts. 89–119. *In* JOYSEY, K. A.
935   and KEMP, T. S. (eds). *Studies in vertebrate evolution.* Oliver and Boyd, Edinburgh, 284
936   pp.

937   CUFF, A. R. and RAYFIELD, E. J. 2013. Feeding mechanics in spinosaurid theropods and
938   extant crocodilians. *PLoS ONE*, **8**, e65295.

939   CUTHBERTSON, R. S., MADDIN, H. C., HOLMES, R. B. and ANDERSON, J. S. 2015.
940   The braincase and endosseous labyrinth of *Plioplatecarpus peckensis* (Mosasauridae,
941   Plioplatecarpinae), with functional implications for locomotor behavior. *The Anatomical
942   Record*, **298**, 1597-1611.

943   DE LA TORRE, S. and SNOWDON, C. T. 2002. Environmental correlates of vocal
944   communication of wild pygmy marmosets, *Cebuella pygmaea. Animal Behaviour*, **63**,
945   847–856.

946   DIAL, B. E. and SCHWENK, K. 1996. Olfaction and predator detection in *Coleonyx brevis*
947   (Squamata: Eublepharidae), with comments on the functional significance of buccal
948   pulsing in geckos. *Journal of Experimental Zoology*, **276**, 415–424.

949   DUIJM, M. J. 1951. On the head posture in birds and its relation features. *Proceedings of the
950   Koninklijke Nederlandse Akademie van Wetenschappen C*, **54**, 202–271.

951   EZCURRA, M. D. 2014. The osteology of the basal archosauromorph *Tasmaniosaurus
952   triassicus* from the Lower Triassic of Tasmania, Australia. *PLoS ONE*, **9**, e86864.

953   EZCURRA, M. D. 2015. *Systematics and evolutionary history of proterosuchian
954   archosauriforms*. PhD thesis, University of Birmingham, UK.

955   EZCURRA, M. D. 2016. The phylogenetic relationships of basal archosauromorphs, with an
956   emphasis on the systematics of proterosuchian archosauriforms. *PeerJ*, **4**, e1778.

957   EZCURRA, M. D. 2017. Can social and sexual selection explain the bizarre snout of
958   proterosuchid archosauriforms?. *Historical Biology*, **29**, 348–358.

959   EZCURRA, M. D. and BUTLER, R. J. 2015a. Taxonomy of the proterosuchid
960   archosauriforms (Diapsida: Archosauromorpha) from the earliest Triassic of South Africa,
961   and implications for the early archosauriform radiation. *Palaeontology*, **58**, 141–170.

962   EZCURRA, M. D. and BUTLER, R. J. 2015b. Post-hatchling cranial ontogeny in the Early
963   Triassic diapsid reptile *Proterosuchus fergusi. Journal of Anatomy*, **226**, 387–402.

964   EZCURRA, M. D. and BUTLER, R. J. 2018. The rise of the ruling reptiles and ecosystem
965   recovery from the Permo-Triassic mass extinction. *Proceedings of the Royal Society B*,
966   **285**, 20180361.

967 EZCURRA, M. D., BUTLER, R. J. and GOWER D. J. 2013. 'Proterosuchia': the origin and
968   early history of Archosauriformes. 9–33. *In* NESBITT S. J., DESOJO, J. B., IRMIS, R.
969   B., (eds). *Phylogeny and palaeobiology of early archosaurs and their kin*. Geological
970   Society of London Special Publication, 379 pp.

971 EZCURRA, M. D., SCHEYER, T. M. and BUTLER, R. J. 2014. The origin and early
972   evolution of Sauria: reassessing the Permian saurian fossil record and the timing of the
973   crocodile-lizard divergence. *PLoS ONE*, **9**, e89165.

974 FABBRI, M., KOCH, N. M., PRITCHARD, A. C., HANSON, M., HOFFMAN, E., BEVER,
975   G. S., BALANOFF, A. M., MORRIS, Z. S., FIELD, D. J., CAMACHO, J., ROWE, T.B.,
976   NORELL, M. A., SMITH, R. M., ABZHANOV, A. and BHULLAR, B. S. 2017. The
977   skull roof tracks the brain during the evolution and development of reptiles including
978   birds. *Nature Ecology & Evolution*, **1**, 1543.

979 FIELD, D. J., LIN, S. C., BEN-ZVI, M., GOLDBOGEN, J. A. and SHADWICK, R. E. 2011.
980   Convergent evolution driven by similar feeding mechanics in balaenopterid whales and
981   pelicans. *The Anatomical Record*, **294**, 1273-1282.

982 FLEMING, I. and GROSS, M. R. 1994. Breeding Competition in a Pacific Salmon (Coho:
983   *Oncorhynchus kisutch*): Measures of Natural and Sexual Selection. *Evolution,* **48**, 637-
984   657.

985 FOFFA, D., CUFF, A. R., SASSOON, J., RAYFIELD, E. J., MAVROGORDATO, M. N. and
986   BENTON, M. J. 2014. Functional anatomy and feeding biomechanics of a giant Upper
987   Jurassic pliosaur (Reptilia: Sauropterygia) from Weymouth Bay, Dorset, UK. *Journal of
988   Anatomy*, **225**, 209-219.

989 FOTH, C., EZCURRA, M. D., SOOKIAS, R. B., BRUSATTE, S. L. and BUTLER, R. J.
990   2016. Unappreciated diversification of stem archosaurs during the Middle Triassic
991   predated the dominance of dinosaurs. *BMC Evolutionary Biology*, **16**, 188.

992 FREEBERG, T. M., DUNBAR, R. I. and ORD, T. J. 2012. Social complexity as a proximate
993   and ultimate factor in communicative complexity. *Philosophical Transactions of the
994   Royal Society of London. Series B, Biological Sciences,* **367,** 1785–1801.

995 FREEBERG, T. M. and KRAMS, I. 2015. Does social complexity link vocal complexity and
996   cooperation? *Journal of Ornithology*, **156**, 125–132.

997 FREITAG, J., LUDWIG, G., ANDREINI, I., RÖSSLER, P. and BREER, H. 1998. Olfactory
998   receptors in aquatic and terrestrial vertebrates. *Journal of Comparative Physiology A*, **183**,
999   635–650.

1000 GARRICK, L. D. and LANG, J. W. 1977. Social signals and behaviors of adult alligators and
1001   crocodiles. *American Zoologist*, **17**, 225–239.

1002 GEORGI, J. A. and SIPLA, J. S. 2008. Comparative and functional anatomy of balance in
1003   aquatic reptiles and birds. 233–256. *In* THEWISSEN J. G. M. and NUMMELA S. (eds).
1004   *Sensory evolution on the threshold: Adaptations in secondarily aquatic vertebrates*.
1005   University of California Press, 358 pp.

GITTLEMAN, J. L. 1991. Carnivore olfactory bulb size: allometry, phylogeny and ecology. *Journal of Zoology*, **225**, 253–272.

GOWER, D. J. and SENNIKOV, A. G. 1996. Endocranial casts of early archosaurian reptiles. *Paläontologische Zeitschrift*, **70**, 579–589.

HAMMER, Ø., HARPER, D. A. T. and RYAN, P. D. 2001. PAST: Paleontological Statistics software package for education and data analysis. *Palaeontologia Electronica*, **4**, 9.

HARMON, L. J., WEIR, J. T., BROCK, C. D., GLOR, R. E. and CHALLENGER, W. 2007. GEIGER: investigating evolutionary radiations. *Bioinformatics*, **24**, 129-131.

HEMILA, S. and REUTER, T. 2008. The physics and biology of olfaction and taste. 29–34. *In* THEWISSEN J. G. M. and NUMMELA S. (eds). *Sensory evolution on the threshold: Adaptations in secondarily aquatic vertebrates*. University of California Press, 358 pp.

HOLLOWAY, W. L., CLAESON, K. M. and O'KEEFE, F. R. 2013. A virtual phytosaur endocast and its implications for sensory system evolution in archosaurs. *Journal of Vertebrate Paleontology*, **33**, 848–857.

HUA, S. and DE BUFFRENIL, V. 1996. Bone histology as a clue in the interpretation of functional adaptations in the Thalattosuchia (Reptilia, Crocodylia). *Journal of Vertebrate Paleontology*, **16**, 703–717.

HULLAR, T. E. 2006. Semicircular canal geometry, afferent sensitivity, and animal behavior. *The Anatomical Record Part A: Discoveries in Molecular, Cellular, and Evolutionary Biology: An Official Publication of the American Association of Anatomists,* **288**, 466-472.

JABLONSKI, D. 1995. Assessing extinction rates. 25–44. *In* MAY, R. M. and LAWTON, J. H. (eds). *Extinction rates*, Oxford University Press, Oxford, 248 pp.

JI, Q., LUO, Z. X., YUAN, C. X. and TABRUM, A. R., 2006. A swimming mammaliaform from the Middle Jurassic and ecomorphological diversification of early mammals. *Science*, **311**, 1123-1127.

JIRAK, D. and JANACEK, J. 2017. Volume of the crocodilian brain and endocast during ontogeny. *PLoS ONE*, **12**, e0178491.

KAWABE, S., SHIMOKAWA, T., MIKI, H., OKAMOTO, T. and MATSUDA, S. 2009. A simple and accurate method for estimating the brain volume of birds: possible application in paleoneurology. *Brain, Behavior and Evolution*, **74**, 295–301.

KAWABE, S., SHIMOKAWA, T., MIKI, H., MATSUDA, S. and ENDO, H. 2013. Variation in avian brain shape: relationship with size and orbital shape. *Journal of Anatomy*, **223**, 495-508.

KLEY, N. J., SERTICH, J. J., TURNER, A. H., KRAUSE, D. W., O'CONNOR, P. M. and GEORGI, J. A. 2010. Craniofacial morphology of *Simosuchus clarki* (Crocodyliformes: Notosuchia) from the Late Cretaceous of Madagascar. *Journal of Vertebrate Paleontology*, **30**, 13–98.

1044   KRAUSE, E. T., KRUGER, O., KOHLMEIER, P. and CASPERS, B. A. 2012. Olfactory kin
1045   recognition in a songbird. *Biology Letters*, **8**, 327–329.

1046   KUNDRÁT, M. 2007. Avian-like attributes of a virtual brain model of the oviraptorid
1047   theropod *Conchoraptor gracilis*. *Naturwissenschaften*, **94**, 499–504.

1048   LAUDER, G. V. and NORTON, S. 1980. Asymmetrical muscle activity during feeding in the
1049   gar, *Lepisosteus oculatus*. *Journal of Experimental Biology*, **84**, 17–32.

1050   LAUTENSCHLAGER, S., RAYFIELD, E. J., ALTANGEREL, P., ZANNO, L. E. and
1051   WITMER, L. M. 2012. The endocranial anatomy of Therizinosauria and its implications
1052   for sensory and cognitive function. *PLoS One*, **7**, e52289.

1053   LAUTENSCHLAGER, S. 2014. Morphological and functional diversity in therizinosaur
1054   claws and the implications for theropod claw evolution. *Proceedings of the Royal Society
1055   of London B: Biological Sciences*, **281**, 20140497.

1056   LAUTENSCHLAGER, S., BRIGHT, J. A. and RAYFIELD, E. J. 2014. Digital dissection–
1057   using contrast-enhanced computed tomography scanning to elucidate hard-and soft-tissue
1058   anatomy in the Common Buzzard *Buteo buteo*. *Journal of Anatomy*, **224**, 412-431.

1059   LAUTENSCHLAGER, S. and BUTLER, R. J., 2016. Neural and endocranial anatomy of
1060   Triassic phytosaurian reptiles and convergence with fossil and modern crocodylians.
1061   *PeerJ*, **4**, e2251.

1062   LAUTENSCHLAGER, S., FERREIRA, G. S. and WERNEBURG, I. 2018. Sensory
1063   evolution and ecology of early turtles revealed by digital endocranial reconstructions.
1064   *Frontiers in Ecology and Evolution,* **6**, 7.

1065   LEAHEY, L. G., MOLNAR, R. E., CARPENTER, K., WITMER, L. M. and SALISBURY,
1066   S. W. 2015. Cranial osteology of the ankylosaurian dinosaur formerly known as *Minmi sp.*
1067   (Ornithischia: Thyreophora) from the Lower Cretaceous Allaru Mudstone of Richmond,
1068   Queensland, Australia. *PeerJ*, **3**, e1475.

1069   LEARDI, J. M., POL, D. and CLARK, J. M. 2017. Detailed anatomy of the braincase of
1070   *Macelognathus vagans* Marsh, 1884 (Archosauria, Crocodylomorpha) using high
1071   resolution tomography and new insights on basal crocodylomorph phylogeny. *PeerJ*, **5**,
1072   e2801.

1073   MALLON, J. C. 2017. Recognizing sexual dimorphism in the fossil record: lessons from
1074   nonavian dinosaurs. *Paleobiology*, **43**, 495–507.

1075   MAREK, R. D., MOON, B. C., WILLIAMS, M. and BENTON, M. J. 2015. The skull and
1076   endocranium of a Lower Jurassic ichthyosaur based on digital reconstructions.
1077   *Palaeontology,* **58**, 723–742.

1078   MARUGÁN-LOBÓN, J., CHIAPPE, L. M. and FARKE, A. A. 2013. The variability of inner
1079   ear orientation in saurischian dinosaurs: testing the use of semicircular canals as a
1080   reference system for comparative anatomy. *PeerJ*, **1**, e124.

1081   MASON, N. A. and BURNS, K. J. 2015. The effect of habitat and body size on the evolution
1082   of vocal displays in Thraupidae (tangers), the largest family of songbirds. *Biological
1083   Journal of the Linnean Society*, **114**, 538–551.

1084 MILIÁN-GARCÍA, Y., VENEGAS-ANAYA, M., FRIAS-SOLER, R., CRAWFORD, A. V.
1085   J., RAMOS-TARGARONA, R., RODRÍGUEZ-SOBERÓN, R., ALONSO-TABET, M.,
1086   THORBIARNARSON, J., SANIUR, O. I., ESPINOSA-LÓPEZ, G. and BERMINGHAM,
1087   E. 2011. Evolutionary history of Cuban crocodiles *Crocodylus rhombifer* and *Crocodylus*
1088   *acutus* inferred from multilocus markers. *Journal of Experimental Zoology Part A*, **315**,
1089   358–375.

1090 MÜLLER, J., BICKELMANN, C. and SOBRAL, G. 2018. The evolution and fossil history of
1091   sensory perception in amniote vertebrates. *Annual Review of Earth and Planetary*
1092   *Sciences*, **46**, 495–519.

1093 NARINS, P. M., FENG, A. S., LIN, W., SCHNITZLER, H. U., DENZINGER, A.,
1094   SUTHERS, R. A. and XU, C. 2004. Old World frog and bird vocalizations contain
1095   prominent ultrasonic harmonics. *The Journal of the Acoustical Society of America*, **115**,
1096   910–913.

1097 NEENAN, J. M. and SCHEYER, T. M. 2012. The braincase and inner ear of *Placodus gigas*
1098   (Sauropterygia, Placodontia)—a new reconstruction based on micro-computed
1099   tomographic data. *Journal of Vertebrate Paleontology*, **32**, 1350–1357.

1100 NEENAN, J. M., REICH, T., EVERS, S. W., DRUCKENMILLER, P. S., VOETEN, D. F.,
1101   CHOINIERE, J. N., BARRETT, P. M., PIERCE, S. E. and BENSON, R. B. 2017.
1102   Evolution of the sauropterygian labyrinth with increasingly pelagic lifestyles. *Current*
1103   *Biology*, **27**, 3852–3858.

1104 NEENAN, J. M., CHAPELLE, K. E., FERNANDEZ, V. and CHOINIERE, J. N. 2019.
1105   Ontogeny of the *Massospondylus* labyrinth: implications for locomotory shifts in a basal
1106   sauropodomorph dinosaur. *Palaeontology*, **62**, 255-265.

1107 NESBITT, S. J. 2011. The early evolution of archosaurs: relationships and the origin of major
1108   clades. *Bulletin of the American Museum of Natural History*, **352**, 1–292.

1109 NESBITT, S. J., STOCKER, M. R., SMALL, B. J. and DOWNS, A. 2009. The osteology and
1110   relationships of *Vancleavea campi* (Reptilia: Archosauriformes). *Zoological Journal of*
1111   *the Linnean Society*, **157**, 814–864.

1112 NICHOLLS, J. A. and GOLDIZEN, A. W. 2006. Habitat type and density influence vocal
1113   signal design in satin bowerbirds. *Journal of Animal Ecology*, **75**, 549–558.

1114 O'BRIEN, H. D., FAITH, J. T., JENKINS, K. E., PEPPE, D. J., PLUMMER, T. W.,
1115   JACOBS, Z. L., LI, B., JOANNES-BOYAU, R., PRICE, G., FENG, Y. X. and TRYON,
1116   C. A. 2016. Unexpected convergent evolution of nasal domes between Pleistocene bovids
1117   and Cretaceous hadrosaur dinosaurs. *Current Biology*, **26**, 503-508.

1118 PARADIS, E., CLAUDE, J. and STRIMMER, K. 2004. APE: analyses of phylogenetics and
1119   evolution in R language. *Bioinformatics*, **20**, 289-290.

1120 PIERCE, S. E., ANGIELCZYK, K. D. and RAYFIELD, E. J. 2008. Patterns of morphospace
1121   occupation and mechanical performance in extant crocodilian skulls: a combined
1122   geometric morphometric and finite element modeling approach. *Journal of morphology*,
1123   **269**, 840–864.

1124 PIERCE, S. E., WILLIAMS, M. and BENSON, R. B. J. 2017. Virtual reconstruction of the
1125　　　endocranial anatomy of the early Jurassic marine crocodylomorph *Pelagosaurus typus*
1126　　　(Thalattosuchia). *PeerJ*, **5**, e3225.

1127 PINHEIRO, F. L., FRANCA, M. A., LACERDA, M. B., BUTLER, R. J. and SCHULTZ, C.
1128　　　L. 2016. An exceptional fossil skull from South America and the origins of the
1129　　　archosauriform radiation. *Scientific Reports*, **6**, 22817.

1130 PINHEIRO, J., BATES, D., DEBROY, S., SARKAR, D. and TEAM, R.C. 2018. NLME:
1131　　　linear and nonlinear mixed effects models. R package version 3.1-137.

1132 PLATT, S. G., RAINWATER, T. R., FINGER, A. G., THORBIARNSARSON, J. B.,
1133　　　ANDERSON, T. A. and MCMURRY, S. T. 2006. Food habits, ontogenetic dietary
1134　　　partitioning and observations of foraging behaviour of Morelet's crocodile (*Crocodylus*
1135　　　*moreletii*) in northern Belize. *The Herpetological Journal*, **16**, 281–290.

1136 POLIHRONAKIS, M. 2006. Morphometric analysis of intraspecific shape variation in male
1137　　　and female genitalia of *Phyllophaga hirticula* (Coleoptera: Scarabaeidae: Melolonthinae).
1138　　　*Annals of the Entomological Society of America*, **99**, 144–150.

1139 PRITZ, M. B. 1975. Anatomical identification of a telencephalic visual area in crocodiles:
1140　　　ascending connections of nucleus rotundus in *Caiman crocodilus*. *Journal of Comparative*
1141　　　*Neurology*, **164**, 323–338.

1142 RAMAJO, L. BALTANÁS, Á., TORRES, R., MANRÍQUEZ, P. H., RODRIGUES-
1143　　　NAVARRO, A. and LAGOS, N. A. 2013. Geographical variation in shell morphology of
1144　　　juvenile snails (*Concholepas concholepas*) along the physical–chemical gradient of the
1145　　　Chilean coast. *Journal of the Marine Biological Association of the United Kingdom*, **93**,
1146　　　2167–2176.

1147 RAUP, D. M. 1979. Size of the Permo-Triassic bottleneck and its evolutionary implications.
1148　　　*Science*, **206**, 217-218.

1149 RAY, S., CHINSAMY, A. and BANDYOPADHYAY, S. 2005. *Lystrosaurus murrayi*
1150　　　(Therapsida, Dicynodontia): bone histology, growth and lifestyle adaptations.
1151　　　*Palaeontology*, **48**, 1169-1185.

1152 RAYFIELD, E. J. and MILNER, A. C. 2008. Establishing a framework for archosaur cranial
1153　　　mechanics. *Paleobiology*, **34**, 494–515.

1154 REIG, O. A. 1970. The Proterosuchia and the early evolution of the archosaurs; an essay
1155　　　about the origin of a major taxon. *Bulletin of the Museum of Comparative Zoology*, **139**,
1156　　　229–292.

1157 RETALLACK, G. J., SMITH, R. M. H. and WARD, P. D. 2003. Vertebrate extinction across
1158　　　Permian–Triassic boundary in Karoo Basin, South Africa. *Geological Society of America*
1159　　　*Bulletin,* **115**, 1133-1152.

1160 REVELL, L. J. 2012. phytools: an R package for phylogenetic comparative biology (and
1161　　　other things). *Methods in Ecology and Evolution*, **3**, 217-223.

1162 ROGERS, S. W. 1998. Exploring dinosaur neuropaleobiology: computed tomography
1163　　　scanning and analysis of an *Allosaurus fragilis* endocast. *Neuron*, **21**, 673–679.

1164   ROHLF, F. 2010. TPSDig2, Version 2.31. New York, NY, Stony Brook.

1165   SALES, M. A. and SCHULTZ, C. L. 2014. Paleoneurology of *Teyumbaita sulcognathus*
1166   (Diapsida: Archosauromorpha) and the sense of smell in rhynchosaurs. *Palaeontologia*
1167   *Electronica*, **17**, 1–10.

1168   SAMPSON, S. D. and WITMER, L. M. 2007. Craniofacial anatomy of *Majungasaurus*
1169   *crenatissimus* (Theropoda: Abelisauridae) from the late Cretaceous of Madagascar.
1170   *Journal of Vertebrate Paleontology*, **27**, 32–102.

1171   SCHELLHORN, R. 2018. A potential link between lateral semicircular canal orientation,
1172   head posture, and dietary habits in extant rhinos (Perissodactyla, Rhinocerotidae). *Journal*
1173   *of Morphology*, **279**, 50-61.

1174   SERENO, P. C. 1991. Basal archosaurs: phylogenetic relationships and functional
1175   implications. *Journal of Vertebrate Paleontology*, **11**, 1–53.

1176   SERENO, P. C., WILSON, J. A., WITMER, L. M., WHITLOCK, J. A., MAGA, A., IDE, O.
1177   and ROWE, T. A. 2007. Structural extremes in a Cretaceous dinosaur. *PLoS ONE*, **2**,
1178   e1230.

1179   SERRANO-MARTÍNEZ, A., KNOLL, F., NARVÁEZ, I., LAUTENSCHLAGER, S. and
1180   ORTEGA, F. 2019. Inner skull cavities of the basal eusuchian *Lohuecosuchus*
1181   *megadontos* (Upper Cretaceous, Spain) and neurosensorial implications. *Cretaceous*
1182   *Research*, **93**, 66-77.

1183   SEWALL, K. B. 2015. Social complexity as a driver of communication and cognition.
1184   *Integrative and Comparative biology*, **55**, 384–395.

1185   SMITH, R. M. H. 1995. Changing fluvial environments across the Permian-Triassic boundary
1186   in the Karoo Basin, South Africa and possible causes of tetrapod extinctions.
1187   *Palaeogeography, Palaeoclimatology, Palaeoecology*, **117**, 81–104.

1188   SMITH, R. M. H. and BOTHA, J. 2005. The recovery of terrestrial vertebrate diversity in the
1189   South African Karoo Basin after the end-Permian extinction. *Comptes Rendus Palevol*, **4**,
1190   623–636.

1191   SMITH, R. M. H. and BOTHA-BRINK, J. 2014. Anatomy of a mass extinction:
1192   sedimentological and taphonomic evidence for drought-induced die-offs at the Permo-
1193   Triassic boundary in the main Karoo Basin, South Africa. *Palaeogeography,*
1194   *Palaeoclimatology, Palaeoecology*, **396**, 99-118.

1195   SMITH, R. M. H. and WARD, P. D. 2001. Pattern of vertebrate extinctions across an event
1196   bed at the Permian-Triassic boundary in the Karoo Basin of South Africa. *Geology*, **29**,
1197   1147–1150.

1198   SMITH, R. M. H., RUBIDGE, B. and VAN DER WALT, M. 2012. Therapsid biodiversity
1199   patterns and palaeoenvironments of the Karoo Basin, South Africa. 31–64. *In*
1200   CHINSAMY-TURAN, A. (ed). *Forerunners of mammals: radiation, histology, biology*.
1201   Indiana University Press, Bloomington. 372 pp.

SOBRAL, G. and MÜLLER, J. 2017. Archosaurs and their kin: the ruling reptiles. 285–326. *In* CLACK, J. A., FAY, R. R., POPPER, A. N. (eds). *Evolution of the Vertebrate Ear*, Springer, 355 pp.

SOBRAL, G., SOOKIAS, R. B., BHULLAR, B. A. S., SMITH, R., BUTLER, R. J. and MÜLLER, J. 2016a. New information on the braincase and inner ear of *Euparkeria capensis* Broom: implications for diapsid and archosaur evolution. *Royal Society Open Science*, **3**, 160072.

SOBRAL, G., REISZ, R., NEENAN, J. M., MÜLLER, J. and SCHEYER, T. M. 2016b. Basal Reptilians, Marine Diapsids, and Turtles: The Flowering of Reptile Diversity. 207–243. *In* CLACK, J. A., FAY, R. R., POPPER, A. N. (eds). *Evolution of the vertebrate ear*. Springer, 355 pp.

STEIGER, S. S., KURYSHEV, V. Y., STENSMYR M. C., KEMPENAERS, B., MUELLER, J. C. 2009. A comparison of reptilian and avian olfactory receptor gene repertoires: species-specific expansion of group γ genes in birds. *BMC Genomics*, **10**, 446.

TATARINOV, L. P. 1961. Pseudosuchians of the USSR. *Paleontologicheskii Zhurnal*, **1961**, 117–132.

TAYLOR, M. P., WEDEL, M. J. and NAISH, D. 2009. Head and neck posture in sauropod dinosaurs inferred from extant animals. *Acta Palaeontologica Polonica*, **54**, 213–220.

THERRIEN, F., HENDERSON, D. M. and RUFF, C. B. 2005. Bite me: Biomechanical models of theropod mandibles and implications for feeding behaviour. 179–237. *In* CARPENTER, K. (ed). *The carnivorous dinosaurs*. Indiana University Press, Bloomington, 371 pp.

TROTTEYN, M. J. and PAULINA-CARABAJAL, A. 2016. Braincase and neuroanatomy of *Pseudochampsa ischigualastensis* and *Tropidosuchus romeri* (Archosauriformes, Proterochampsia). *Ameghiniana*, **53**, 527–542.

VERGNE, A. L., PRITZ, M. B. and MATHEYON, N. 2009. Acoustic communication in crocodilians: from behaviour to brain. *Biological Reviews*, **84**, 391-411.

VIDAL, D., ORTEGA, F. and SANZ, J. L. 2014. Titanosaur osteoderms from the Upper Cretaceous of Lo Hueco (Spain) and their implications on the armor of Laurasian titanosaurs. *PLoS ONE*, **9**, e102488.

VIGLIETTI, P. A., SMITH, R. M. and COMPTON, J. S. 2013. Origin and palaeoenvironmental significance of *Lystrosaurus* bonebeds in the earliest Triassic Karoo Basin, South Africa. *Palaeogeography, Palaeoclimatology, Palaeoecology*, **392**, 9–21.

VULLO, R., ALLAIN, R. and CAVIN, L. 2016. Convergent evolution of jaws between spinosaurid dinosaurs and pike conger eels. *Acta Palaeontologica Polonica*, **61**, 825-829.

WALSH, S. A., BARRETT, P. M., MILNER, A. C., MANLEY, G. and WITMER, L. M. 2009. Inner ear anatomy is a proxy for deducing auditory capability and behaviour in reptiles and birds. *Proceedings of the Royal Society of London B: Biological Sciences*, **276,** 1355–1360.

1241 WALSH, S. A., LUO, Z. X. and BARRETT, P. M. 2013. Modern imaging techniques as a
1242   window to prehistoric auditory worlds. 227-261. *In* KOPPL, C., MANLEY, G., POPPER,
1243   A. N. and FAY, R. R. (eds). *Insights from Comparative Hearing Research.* Springer, 396
1244   pp.

1245 WELDON, P. J., SWENSON, D. J., OLSON, J. K. and BRINKMEIER, W. G. 1990. The
1246   American alligator detects food chemicals in aquatic and terrestrial environments.
1247   *Ethology*, **85**, 191–198.

1248 WELMAN, J. 1998. The taxonomy of the South African proterosuchids (Reptilia,
1249   Archosauromorpha). *Journal of Vertebrate Paleontology*, **18**, 340–347.

1250 WHARTON, D. S. 2000. An enlarged endocranial venous system in *Steneosaurus*
1251   *pictaviensis* (Crocodylia: Thalattosuchia) from the Upper Jurassic of Les Lourdines,
1252   France. *Comptes Rendus de l'Académie des Sciences-Series IIA-Earth and Planetary*
1253   *Science*, **331**, 221–226.

1254 WITMER, L. M. and RIDGELY, R. C. 2009. New insights into the brain, braincase, and ear
1255   region of tyrannosaurs (Dinosauria, Theropoda), with implications for sensory
1256   organization and behavior. *The Anatomical Record*, **292**, 1266–1296.

1257 WITMER, L. M., CHATTERJEE, S., FRANZOSA, J. and ROWE, T. 2003. Neuroanatomy of
1258   flying reptiles and implications for flight, posture and behaviour. *Nature*, **425**, 950–953.

1259 WITMER, L. M., RIDGELY, R. C., DUFEAU, D. L. and SEMONES, M. C. 2008. Using CT
1260   to peer into the past: 3D visualization of the brain and ear regions of birds, crocodiles, and
1261   nonavian dinosaurs. 67–87. *In* ENDO, H. and FREY, R. (eds). *Anatomical imaging:*
1262   *towards a new morphology.* Springer, 110 pp.

1263 YI, H. and NORELL, M. A. 2015. The burrowing origin of modern snakes. *Science*
1264   *Advances*, **1**, e1500743.

1265 ZAHAVI, A. 1975. Mate selection—a selection for a handicap. *Journal of Theoretical*
1266   *Biology*, **53**, 205–214.

1267 ZAHAVI, A. 1977. The cost of honesty: further remarks on the handicap principle. *Journal of*
1268   *Theoretical Biology*, **67**, 603–605.

1269 ZELENITSKY, D. K., THERRIEN, F. and KOBAYASHI, Y. 2009. Olfactory acuity in
1270   theropods: palaeobiological and evolutionary implications. *Proceedings of the Royal*
1271   *Society of London B: Biological Sciences*, **276**, 667–673.

1272

1273

1274

1275 FIG 1. Specimens of *Proterosuchus fergusi* analysed in this study. A–D, SNSB-BSPG 1934

1276 VIII 514; E–H, RC 846 (proposed neotype). Skulls are shown as photographs in dorsal (A, E),

1277 right lateral (B, F), and left lateral (C, G) views, with outline drawings (D, H) of the most

1278 complete lateral view. Outline drawing of RC 846 (H) is taken from Ezcurra & Butler

1279 (2015a). All scale bars equal 50 mm.

1280

1281 FIG 2. Brain endocast reconstructions of *Proterosuchus fergusi*. (A–B) SNSB-BSPG 1934

1282 VIII 514; (C–D) RC 846; (E–F) RC 846 μCT. Reconstructions show dorsal views of

1283 endocasts in situ (A, C, E), dorsal and left lateral views of isolated endocasts (B, D, F).

1284 Abbreviations: ca, carotid artery canal; cb, cerebellum; ch, cerebral hemispheres; el,

1285 endosseous labyrinth; mcv, middle cerebral vein; mo, medulla oblongata; ob, olfactory bulb;

1286 ot, olfactory tract; iv, trochlear nerve canal; v, trigeminal nerve canal; vi, abducens nerve; vii,

1287 facial nerve canal. Colour key: cranial endocast (blue); endosseous labyrinth (pink); cranial

1288 nerves (yellow); arterial canals (red); smaller venous canals (dark blue). Scale bars: 50 mm

1289 (A, C); 25 mm (E); 10 mm (B, D, F).

1290

1291 FIG 3. Endosseous labyrinths of *Proterosuchus fergusi* from highest to lowest CT resolution.

1292 A, B, left (A) and right (B) labyrinths of RC 846 (μCT). C, D, left (C) and right (D) labyrinths

1293 of SNSB-BSPG 1934 VIII 514. E, F, left (E) and right (F) labyrinths of RC 846. Labyrinths

1294 are shown in (from left to right) lateral, dorsal, medial, anterior and posterior views.

1295 Abbreviations: asc, anterior semi-circular canal; cc, crus communis; ecd, endosseous cochlear

1296 duct; fv, fenestra vestibuli; lsc, lateral semi-circular canal; psc, posterior semi-circular canal.

1297 All scale bars equal 5 mm.

1298

1299 FIG 4. Morphospace plots of archosauriform brain outlines based on elliptic Fourier analysis

1300 and after principal component analysis. Abbreviations: NAAR, non-archosaurian

1301   archosauriform; NPPS, non-phytosaurian pseudosuchians; PHYT, Phytosauria; PTER,

1302   Pterosauria; SAUR, Sauropodomorpha; ORTH, Ornithischia; NATH, non-avian theropods;

1303   AVES, Aves. † denotes extinct taxa. For taxonomic information see Brown *et al*. (2019, Fig.

1304   S9). Silhouettes used include work by S. Hartman, M. Witton, N. Tamura and T. M. Keesey

1305   (see http://phylopic.org for full licensing information).

1306

1307   FIG 5. Morphospace plots of avian and reptile inner ear outlines based on elliptic Fourier

1308   analysis and after principal component analysis, both with and without the endosseous

1309   cochlear duct (ECD). (A) with ECD; (B) without ECD. Colour key: Aquatic (dark blue);

1310   Semi-aquatic (light blue); Terrestrial (yellow). Abbreviations: SQUA, Squamata; SAUO,

1311   Sauropterygia; TEST, Testudines; NAAR, non-archosaurian archosauriform; PHYT,

1312   Phytosauria; NPPS, non-phytosaurian pseudosuchians; ORNI, Ornithischia; SAUR,

1313   Sauropodomorpha; NATH, non-avian theropods; AVES, Aves. For taxonomic information

1314   see Brown *et al*. (2019, Fig. S6).

1315

1316   FIG 6. Morphospace plots of avian and reptile semi-circular canal landmarks after principal

1317   component analysis. PC1 versus PC2. (A) ASC; (B) LSC; (C) PSC. For taxonomic

1318   information see Brown *et al*. (2019, fig. S9).

1319

1320   FIG 7. Discerning the 'alert' head posture in life from the orientation of the lateral semi-

1321   circular canal (LSC). (A) Orientation of the LSC when head posture of *Proterosuchus fergusi*

1322   is horizontal in both specimens studied. (B) Head posture of *P. fergusi* in life following mean

1323   average orientation of all LSC planes studied. (C) Comparative head posture of *Crocodylus*

1324   *johnstoni* following the orientation of the LSC plane (Witmer *et al*. 2008). *Proterosuchus*

1
2
3
4
5
6
7
8
9
10
11
12
13
14
15
16
17
18
19
20
21
22
23
24
25
26
27
28
29
30
31
32
33
34
35
36
37
38
39
40
41
42
43
44
45
46
47
48
49
50
51
52
53
54
55
56
57
58
59
60

1325 *fergusi* and *C. johnstoni* skull figures modified from Ezcurra & Butler (2015a) and Witmer *et*

1326 *al.* (2008) respectively.

1327

1328 FIG 8. Correlation plot between scaled/log transformed ECD length and variables of hearing

1329 sensitivity for extant reptiles and Aves. Both a linear regression (solid line) and PGLS

1330 regression (dashed line) were used to estimate the auditory capabilities of *Proterosuchus*

1331 *fergusi* (indicated by the hollow circle). Sensitivity variables: (A) mean hearing frequency;

1332 (B) hearing range. Abbreviations: SQUA, Squamata; RHYN, Rhynchocephalia; TEST,

1333 Testudines; CROC, Crocodylomorpha; AVES, Aves. For taxonomic information see Brown

1334 *et al.* (2019, fig. S10).

1335

1336 FIG 9. Change in the resistance to dorsoventral bending (lx), mediolateral bending (ly), and

1337 torsion (J) along the rostra in *Proterosuchus fergusi* and comparative extant taxa. (A) log lx

1338 true size; (B) log lx scaled size; (C) log ly true size; (D) log ly scaled size; (E) log J true size;

1339 (F) log J scaled size. In *Proterosuchus fergusi*, both a straight beam (solid line) and a curved

1340 beam (dashed line) were used when analysing the anterior 20% of the rostrum.

1341

1342 FIG 10. Evolution of the brain cavity in Archosauriformes. Left lateral view of the brain

1343 cavity of saurians redrawn from the literature. (A) snake *Dispholidus typus* (Allemand *et al.*

1344 2017); (B) *Proterosuchus fergusi* (this study); (C) proterochampsian *Tropidosuchus romeri*

1345 (Trotteyn & Paulina-Carabajal 2016); (D) *Parasuchus angustifrons* (retrodeformed,

1346 Lautenschlager & Butler 2016); (E) *Ebrachosuchus neukami* (retrodeformed, Lautenschlager

1347 & Butler 2016); (F) *Riojasuchus tenuisceps* (Baczko & Desojo 2016); (G) *Pelagosaurus typus*

1348 (Pierce *et al.* 2017); (H) *Caiman crocodilus* (Jirak & Janacek 2017); (I) *Crocodylus seamensis*

1349   (Kawabe *et al.* 2009); (J) *Anhanguera santanae* (Witmer *et al.* 2003); (K) *Tyrannosaurus rex*

1350   (Witmer *et al.* 2008); (L) *Bubo virginianus* (Witmer *et al.* 2008). † denotes extinct taxa.

1351   Phylogeny following Nesbitt (2011) and Ezcurra (2016). Brain cavities not to scale.

1352

1353   FIG 11. Evolution of the endosseous labyrinth in Archosauriformes. Lateral view of the left

1354   labyrinth of archosauriforms redrawn from the literature. (A) snake *Ptyas mucosa* (reversed,

1355   Yi & Norell 2015); (B) *Proterosuchus fergusi* (this study); (C) proterochampsian

1356   *Tropidosuchus romeri* (reversed, Trotteyn & Paulina-Carabajal 2016); (D) *Euparkeria*

1357   *capensis* (reversed, Sobral *et al.* 2016); (E) *Parasuchus angustifrons* (retrodeformed,

1358   Lautenschlager & Butler 2016); (F) *Ebrachosuchus neukami* (retrodeformed, Lautenschlager

1359   & Butler 2016); (G) *Simosuchus clarki* (reversed, Kley 2010); (H) *Pelagosaurus typus* (Pierce

1360   *et al.* 2017); (I) *Steneosaurus cf. gracilirostris* (Brusatte *et al.* 2016); (J) *Crocodylus johnstoni*

1361   (Brusatte *et al.* 2016); (K) *Alligator mississippiensis* (Brusatte *et al.* 2016); (L) *Stegosaurus*

1362   *stenops* (Leahey *et al.* 2015); (M) *Camarasaurus lentus* (Witmer *et al.* 2008); (N)

1363   *Tyrannosaurus rex* (Witmer *et al.* 2008); (O) *Bubo virginianus* (Witmer *et al.* 2008). †

1364   denotes extinct taxa. Abbreviations: ASC, anterior semi-circular canal; ECD, endosseous

1365   cochlea duct; LSC, lateral semi-circular canal; PSC, posterior semi-circular canal. Phylogeny

1366   following Nesbitt (2011), Ezcurra (2016) and Leardi *et al.* (2017). Labyrinths not to scale.

1367

1368   Table 1. Results of one-way PERMANOVA test on endocranial outlines between ecological
1369   groupings using all axes. *Proterosuchus* is excluded. Results in bold show statistical
1370   significance at p = 0.05.

1371   Permutation N   10000

1372   Total sum of squares   6.193

1373   Within-group sum of squares   5.098

1374   F   7.082

1375   p   0.0002

Ecological groupings	p-value (w/ ECD)
Aquatic/Semi-aquatic	0.0998
Aquatic/Terrestrial	0.4222
Semi-aquatic/Terrestrial	**<0.0001**

1376

1377 Table 2. Results of one-way PERMANOVA test on endocranial outlines between
1378 phylogenetic groupings and using all axes. Abbreviations: NAAR, non-archosaurian
1379 archosauriform; PHYT, Phytosauria; NPPS, non-phytosaurian pseudosuchians; PTER,
1380 Pterosauria; ORTH, Ornithischia; SAUR, Sauropodomorpha; NATH, non-avian theropods;
1381 AVES, Aves. Results in bold show statistical significance at p = 0.05.

1382 Permutation N   10000

1383 Total sum of squares 6.255

1384 Within-group sum of squares   2.825

1385 F   10.75

1386 p   1.00E-04

p-values	PHYT	NPPS	PTER	ORNI	SAUR	NATH	AVES
NAAR	0.4312	0.7721	0.104	**0.0215**	**0.0190**	0.0612	**0.0064**
PHYT		0.1084	**0.0183**	**0.0043**	**0.0033**	**0.0175**	**0.0002**
NPPS			**0.0015**	**0.0001**	**0.0001**	**0.0002**	**0.0001**
PTER				**0.0126**	**0.0310**	**0.0136**	**0.0406**
ORNI					**0.0086**	**0.0263**	**0.0001**
SAUR						**0.0014**	**0.0001**
NATH							**0.0001**

1387

1388

1389

1390 Table 3. Results of one-way PERMANOVA test on inner ear outlines between ecological
1391 groupings with (left) and without (right) the endosseous cochlea duct (ECD) and using all
1392 axes. *Proterosuchus* is excluded. Results in bold show statistical significance at p = 0.05.

1393 Permutation N   10000/10000

1394 Total sum of squares 7.52/ 5.685

1395 Within-group sum of squares   6.546/ 5.315

1396 F   6.772/ 3.345

1397 p   0.0001/ 0.0044

Ecological groupings	p-value (w/ ECD)	p-value (w/o ECD)
Aquatic/Semi-aquatic	**0.0099**	**0.0282**
Aquatic/Terrestrial	**0.0003**	**0.0013**
Semi-aquatic/Terrestrial	**0.0099**	0.2968

1398

1399 Table 4. Results of one-way PERMANOVA test on inner ear outlines between phylogenetic
1400 groupings with (left) and without (right) the endosseous cochlea duct (ECD) and using all

1401 axes. Abbreviations: SQUA, Squamata; SAUO, Sauropterygia; TEST, Testudines; NAAR,
1402 non-archosaurian archosauriform; PHYT, Phytosauria; NPPS, non-phytosaurian
1403 pseudosuchians; ORNI, Ornithischia; SAUR, Sauropodomorpha; NATH, non-avian
1404 theropods; AVES, Aves. Results in bold show statistical significance at p = 0.05.

1405 Permutation N   10000

1406 Total sum of squares   1.658

1407 Within-group sum of squares   0.522

1408 F   10.26

1409 p   9.999E-05

p-values (w/o ECD \ w/ ECD)	SQUA	SAUO	TEST	NAAR	PHYT	NPPS	ORNI	SAUR	NATH	AVES
SQUA		**0.0002**	**0.0005**	**0.0010**	**0.0065**	**0.0001**	**0.0005**	**0.0001**	**0.0001**	**0.0001**
SAUO	**0.0101**		0.4432	0.2562	0.1680	**0.0002**	**0.0015**	**0.0001**	**0.0001**	**0.0001**
TEST	**0.0032**	**0.0307**		0.1189	0.1078	**0.0001**	**0.0014**	**0.0001**	**0.0001**	**0.0001**
NAAR	**0.0303**	0.3823	**0.0007**		0.0995	**0.0027**	**0.0290**	**0.0034**	**0.0014**	**0.0007**
PHYT	0.2860	0.6812	**0.0320**	0.7363		0.0671	0.1380	**0.0150**	**0.0119**	**0.0040**
NPPS	**0.0392**	0.3248	**0.0185**	0.1340	0.6042		**0.0023**	**0.0001**	**0.0001**	**0.0001**
ORNI	**0.0028**	0.3494	**0.0002**	**0.0063**	**0.0392**	**0.0072**		0.2123	**0.0080**	**0.0013**
SAUR	**0.0003**	**0.0200**	**0.0001**	0.0618	0.1232	**0.0001**	**0.0005**		0.1188	**0.0015**
NATH	**0.0001**	**0.0003**	**0.0001**	**0.0047**	**0.0162**	**0.0001**	**0.0001**	**0.0319**		**0.0011**
AVES	**0.0001**	**0.0001**	**0.0001**	**0.0004**	**0.0053**	**0.0001**	**0.0001**	**0.0001**	**0.0001**	

1410

1411 Table 5. Results of canonical variate analysis on semi-circular canal landmarks using all axes.
1412 *Proterosuchus* was excluded. Results in bold show statistical significance at p = 0.05.

1413 Permutation N   10000

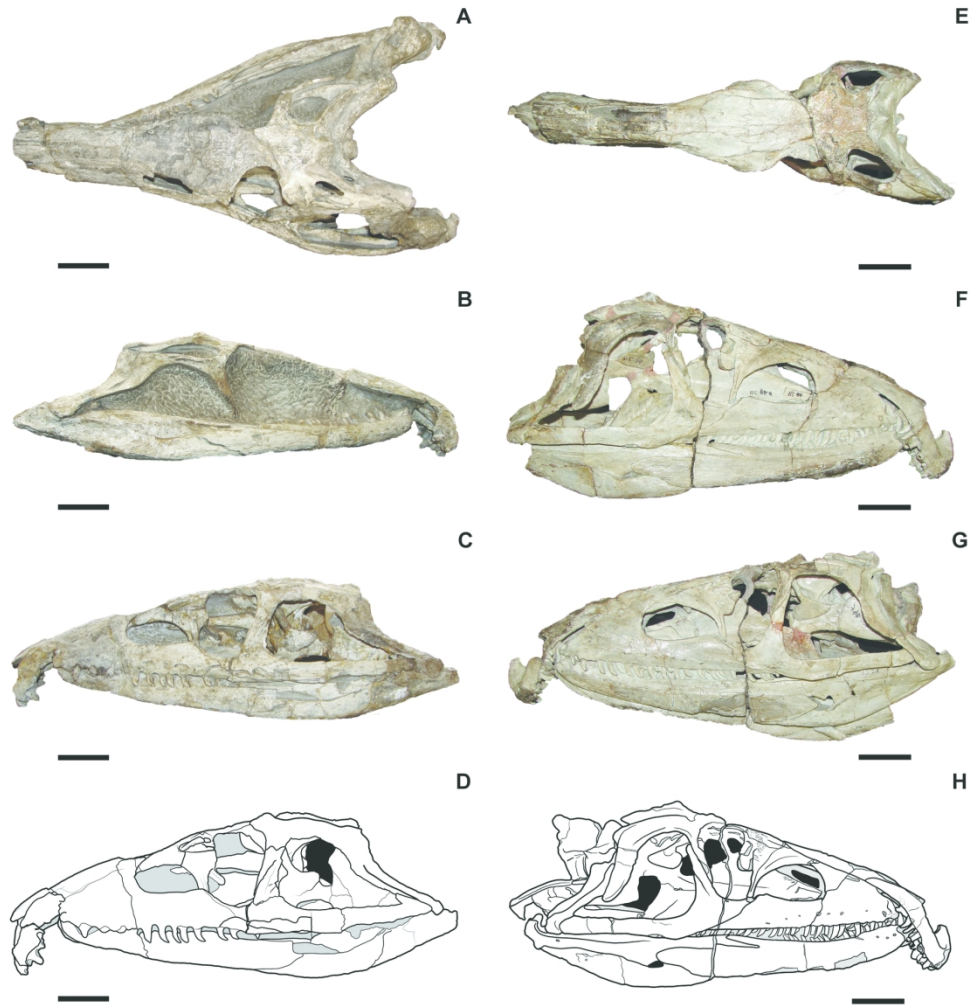| Ecological groupings	ASC		LSC		PSC	
	Procrustes	**p-value**	**Procrustes**	**p-value**	**Procrustes**	**p-value**
Terrestrial/Semi-Aquatic	0.1937	**0.0146**	0.1093	0.2442	0.1921	**0.0178**
Terrestrial/Aquatic	0.2970	**0.0002**	0.2646	**0.0050**	0.2168	**0.0051**
Semi-Aquatic/Aquatic	0.1655	**0.0075**	0.1778	**0.0314**	0.1099	0.3103

1414

1415

1416

FIG 1. Specimens of Proterosuchus fergusi analysed in this study. A–D, SNSB-BSPG 1934 VIII 514; E–H, RC 846 (proposed neotype). Skulls are shown as photographs in dorsal (A, E), right lateral (B, F), and left lateral (C, G) views, with outline drawings (D, H) of the most complete lateral view. Outline drawing of RC 846 (H) is taken from Ezcurra & Butler (2015a). All scale bars equal 50 mm.
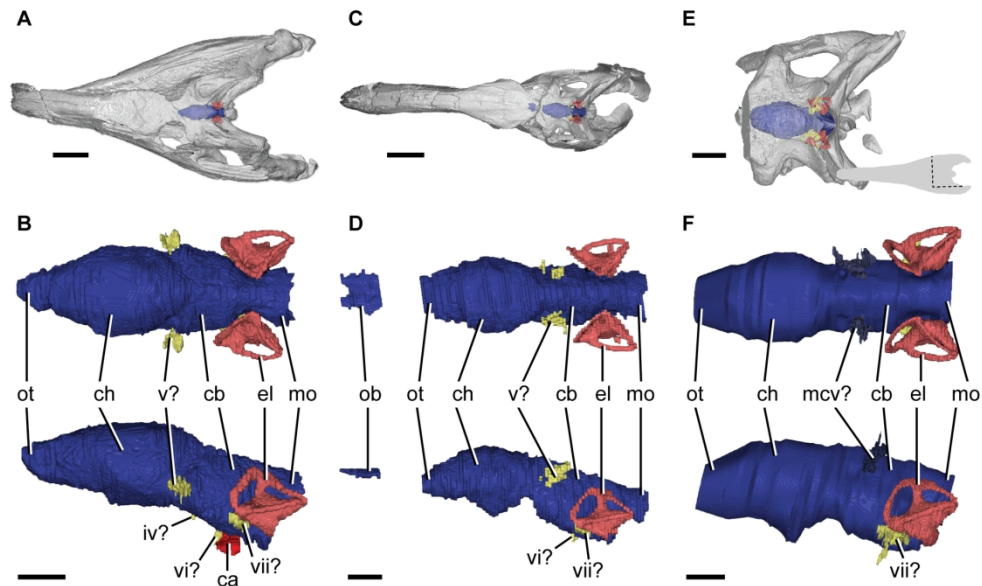
165x170mm (300 x 300 DPI)

FIG 2. Brain endocast reconstructions of Proterosuchus fergusi. (A–B) SNSB-BSPG 1934 VIII 514; (C–D) RC 846; (E–F) RC 846 μCT. Reconstructions show dorsal views of endocasts in situ (A, C, E), dorsal and left lateral views of isolated endocasts (B, D, F). Abbreviations: ca, carotid artery canal; cb, cerebellum; ch, cerebral hemispheres; el, endosseous labyrinth; mcv, middle cerebral vein; mo, medulla oblongata; ob, olfactory bulb; ot, olfactory tract; iv, trochlear nerve canal; v, trigeminal nerve canal; vi, abducens nerve; vii, facial nerve canal. Colour key: cranial endocast (blue); endosseous labyrinth (pink); cranial nerves (yellow); arterial canals (red); smaller venous canals (dark blue). Scale bars: 50 mm (A, C); 25 mm (E); 10 mm (B, D, F).
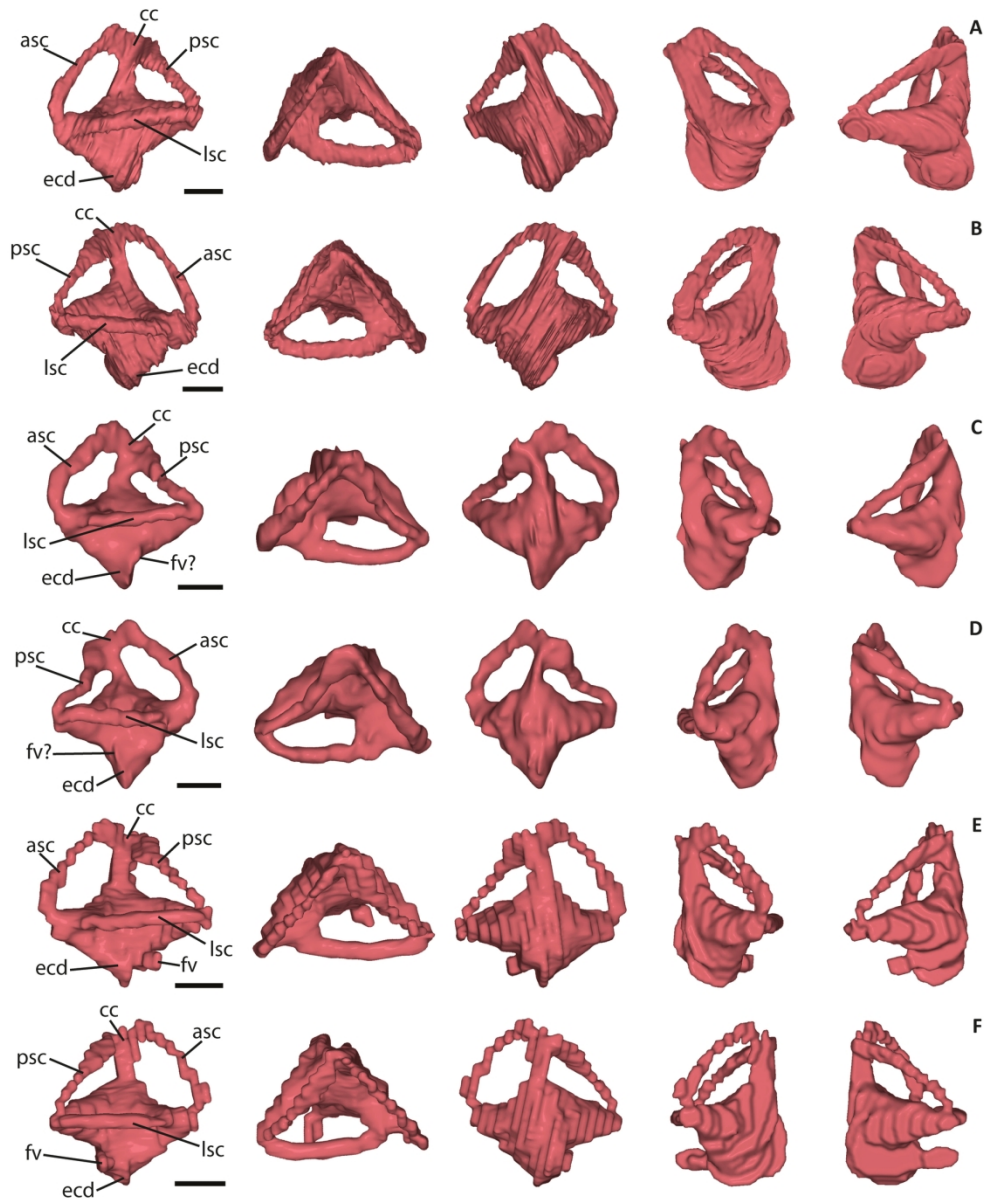
170x100mm (300 x 300 DPI)

FIG 3. Endosseous labyrinths of Proterosuchus fergusi from highest to lowest CT resolution. A, B, left (A) and right (B) labyrinths of RC 846 (µCT). C, D, left (C) and right (D) labyrinths of SNSB-BSPG 1934 VIII 514. E, F, left (E) and right (F) labyrinths of RC 846. Labyrinths are shown in (from left to right) lateral, dorsal, medial, anterior and posterior views. Abbreviations: asc, anterior semi-circular canal; cc, crus communis; ecd, endosseous cochlear duct; fv, fenestra vestibuli; lsc, lateral semi-circular canal; psc, posterior semi-circular canal. All scale bars equal 5 mm.
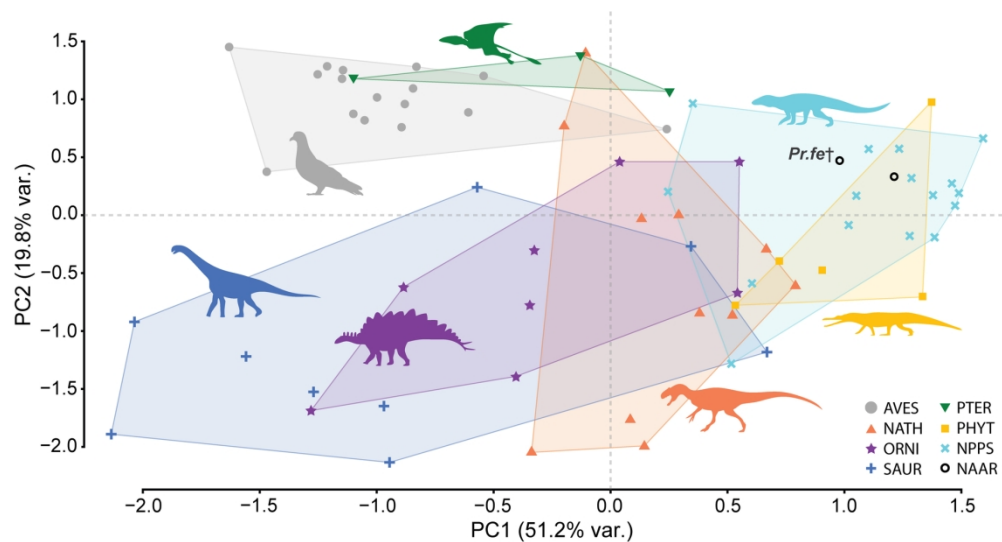
161x194mm (300 x 300 DPI)

FIG 4. Morphospace plots of archosauriform brain outlines based on elliptic Fourier analysis and after principal component analysis. Abbreviations: NAAR, non-archosaurian archosauriform; NPPS, non-phytosaurian pseudosuchians; PHYT, Phytosauria; PTER, Pterosauria; SAUR, Sauropodomorpha; ORTH, Ornithischia; NATH, non-avian theropods; AVES, Aves. † denotes extinct taxa. For taxonomic information see Brown et al. (2019, Fig. S9). Silhouettes used include work by S. Hartman, M. Witton, N. Tamura and T. M. Keesey (see http://phylopic.org for full licensing information).
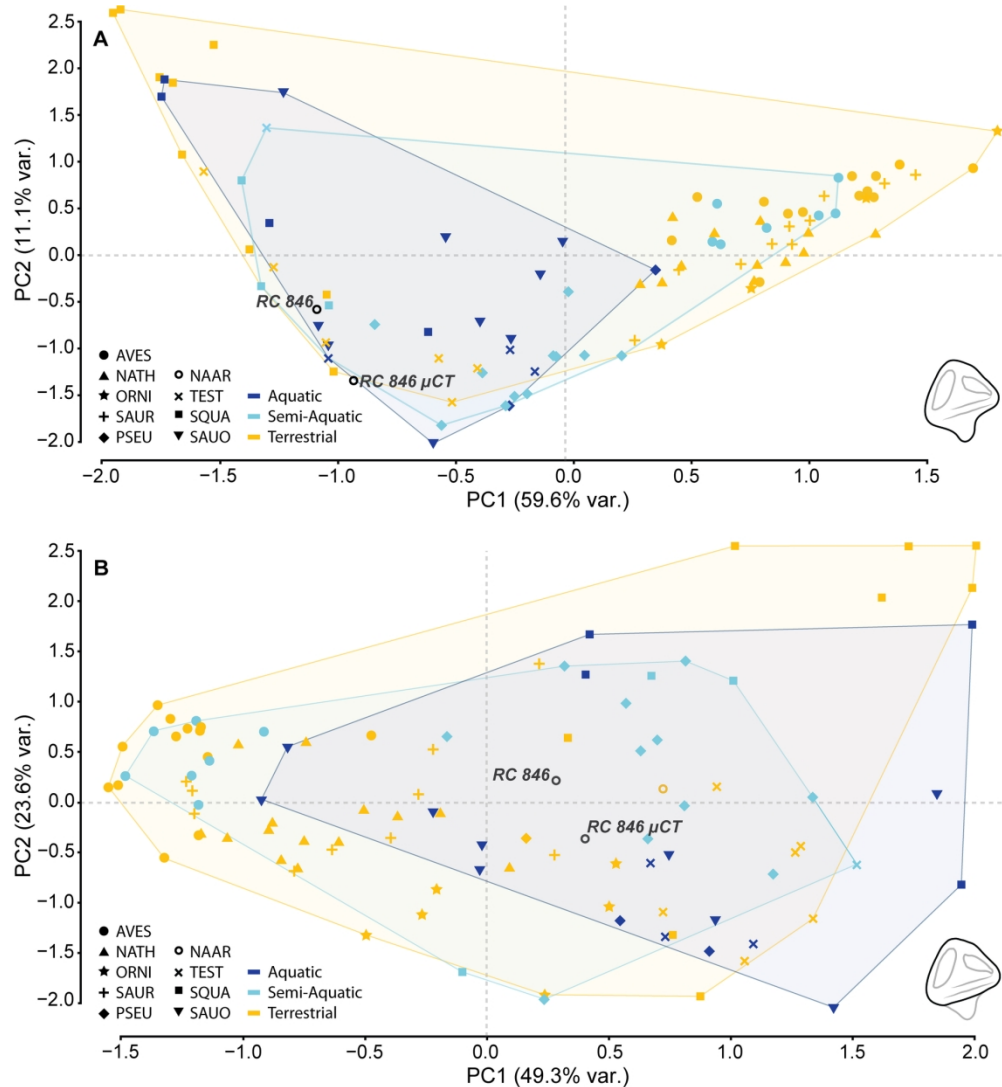
166x88mm (300 x 300 DPI)

FIG 5. Morphospace plots of avian and reptile inner ear outlines based on elliptic Fourier analysis and after principal component analysis, both with and without the endosseous cochlear duct (ECD). (A) with ECD; (B) without ECD. Colour key: Aquatic (dark blue); Semi-aquatic (light blue); Terrestrial (yellow). Abbreviations: SQUA, Squamata; SAUO, Sauropterygia; TEST, Testudines; NAAR, non-archosaurian archosauriform; PHYT, Phytosauria; NPPS, non-phytosaurian pseudosuchians; ORNI, Ornithischia; SAUR, Sauropodomorpha; NATH, non-avian theropods; AVES, Aves. For taxonomic information see Brown et al. (2019, Fig. S6).
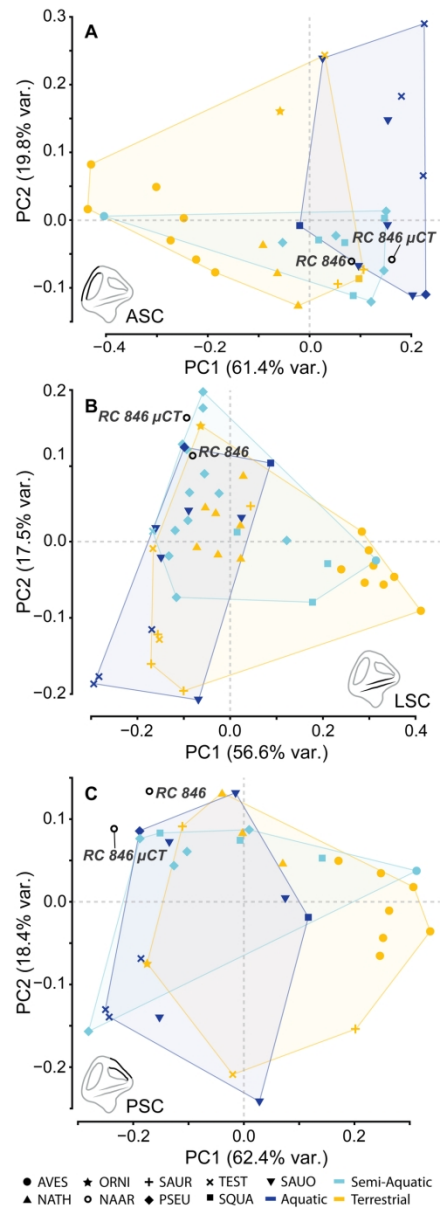
166x180mm (300 x 300 DPI)

FIG 6. Morphospace plots of avian and reptile semi-circular canal landmarks after principal component analysis. PC1 versus PC2. (A) ASC; (B) LSC; (C) PSC. For taxonomic information see Brown et al. (2019, fig. S9).
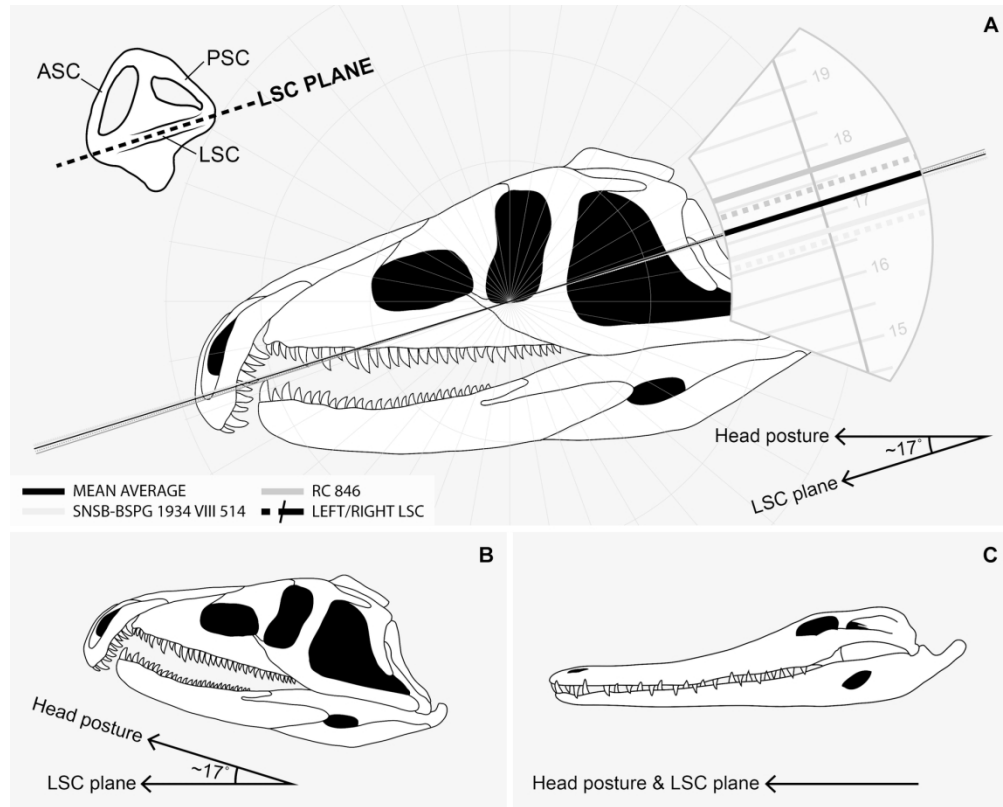
80x226mm (300 x 300 DPI)

FIG 7. Discerning the 'alert' head posture in life from the orientation of the lateral semi-circular canal (LSC). (A) Orientation of the LSC when head posture of Proterosuchus fergusi is horizontal in both specimens studied. (B) Head posture of P. fergusi in life following mean average orientation of all LSC planes studied. (C) Comparative head posture of Crocodylus johnstoni following the orientation of the LSC plane (Witmer et al. 2008). Proterosuchus fergusi and C. johnstoni skull figures modified from Ezcurra & Butler (2015a) and Witmer et al. (2008) respectively.

165x133mm (300 x 300 DPI)

1
2
3
4
5
6
7
8
9
10
11
12
13
14
15
16
17
18
19
20
21
22
23
24
25
26
27
28
29
30
31
32
33
34
35
36
37
38
39
40
41
42
43
44
45
46
47
48
49
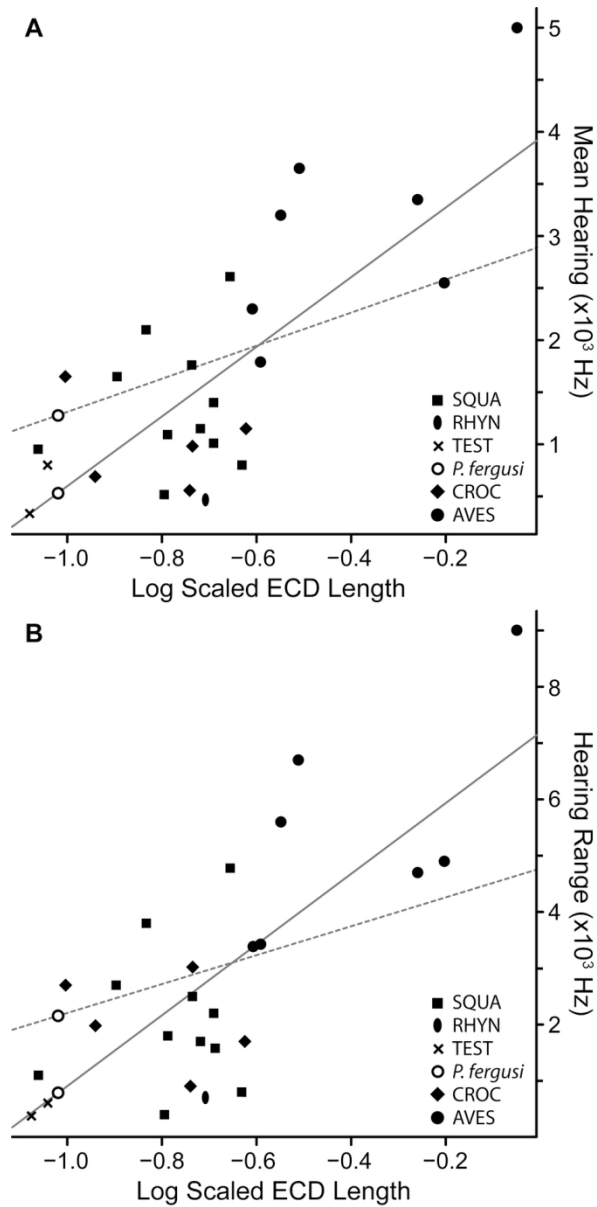50
51
52
53
54
55
56
57
58
59
60

FIG 8. Correlation plot between scaled/log transformed ECD length and variables of hearing sensitivity for extant reptiles and Aves. Both a linear regression (solid line) and PGLS regression (dashed line) were used to estimate the auditory capabilities of Proterosuchus fergusi (indicated by the hollow circle). Sensitivity variables: (A) mean hearing frequency; (B) hearing range. Abbreviations: SQUA, Squamata; RHYN, Rhynchocephalia; TEST, Testudines; CROC, Crocodylomorpha; AVES, Aves. For taxonomic information see Brown et al. (2019, fig. S10).
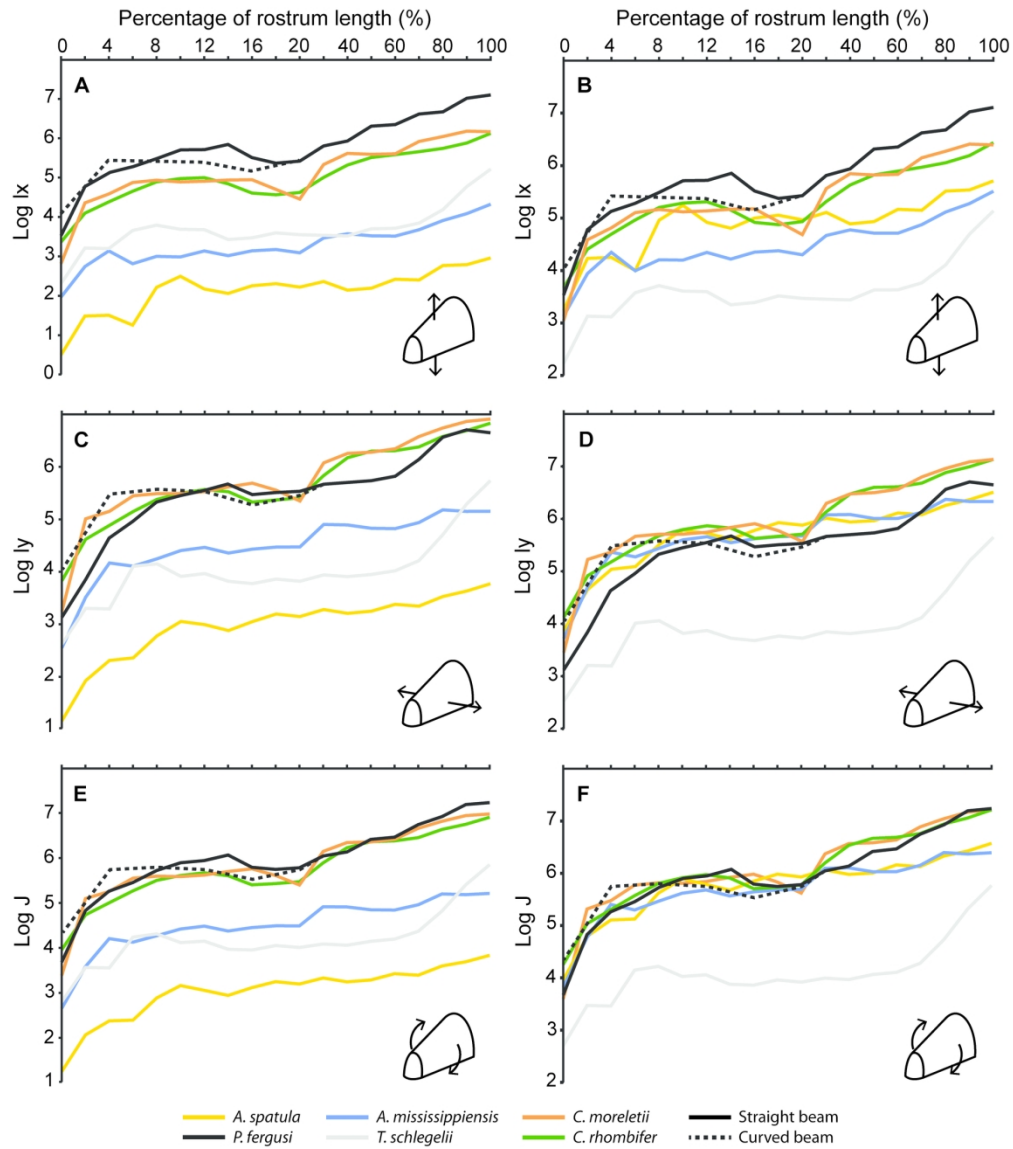
81x165mm (300 x 300 DPI)

1
2
3
4
5
6
7
8
9
10
11
12
13
14
15
16
17
18
19
20
21
22
23
24
25
26
27
28
29
30
31
32
33
34
35
36
37
38
39
40
41
42
43
44
45
46
47
48
49
50
51
52
53
54
55
56
57
58
59
60

FIG 9. Change in the resistance to dorsoventral bending (Ix), mediolateral bending (Iy), and torsion (J) along the rostra in Proterosuchus fergusi and comparative extant taxa. (A) log Ix true size; (B) log Ix scaled size; (C) log Iy true size; (D) log Iy scaled size; (E) log J true size; (F) log J scaled size. In Proterosuchus fergusi, both a straight beam (solid line) and a curved beam (dashed line) were used when analysing the anterior 20% of the rostrum.
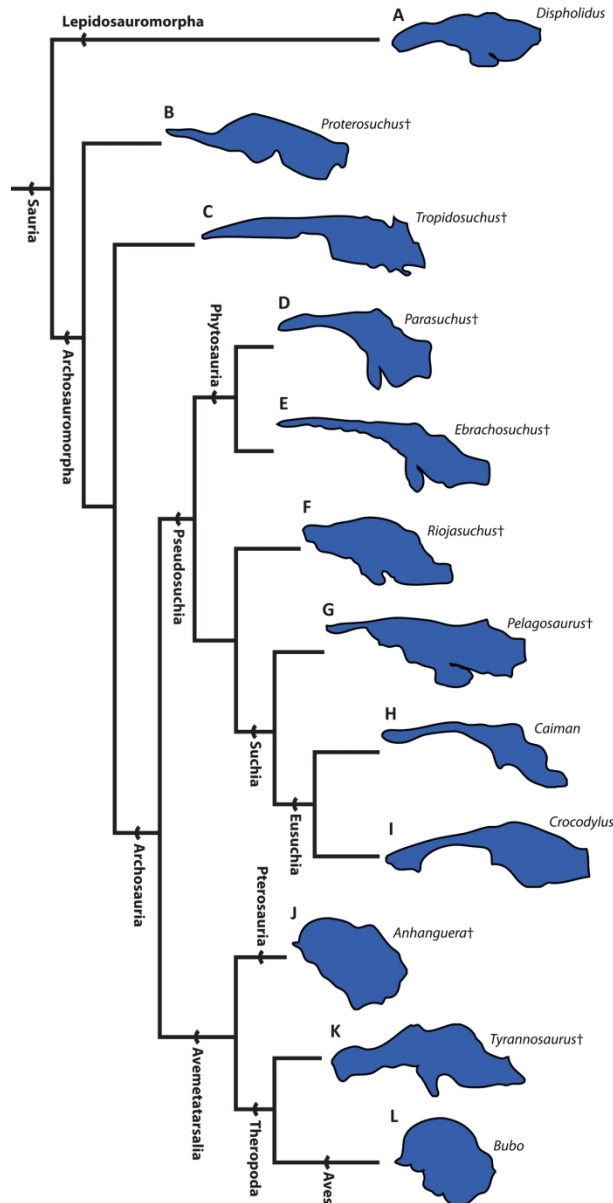
166x189mm (300 x 300 DPI)

1
2
3
4
5
6
7
8
9
10
11
12
13
14
15
16
17
18
19
20
21
22
23
24
25
26
27
28
29
30
31
32
33
34
35
36
37
38
39
40
41
42
43
44
45
46
47
48
49
50
51
52
53
54
55
56
57
58
59
60

FIG 10. Evolution of the brain cavity in Archosauriformes. Left lateral view of the brain cavity of saurians redrawn from the literature. (A) snake Dispholidus typus (Allemand et al. 2017); (B) Proterosuchus fergusi (this study); (C) proterochampsian Tropidosuchus romeri (Trotteyn & Paulina-Carabajal 2016); (D) Parasuchus angustifrons (retrodeformed, Lautenschlager & Butler 2016); (E) Ebrachosuchus neukami (retrodeformed, Lautenschlager & Butler 2016); (F) Riojasuchus tenuisceps (Baczko & Desojo 2016); (G) Pelagosaurus typus (Pierce et al. 2017); (H) Caiman crocodilus (Jirak & Janacek 2017); (I) Crocodylus seamensis (Kawabe et al. 2009); (J) Anhanguera santanae (Witmer et al. 2003); (K) Tyrannosaurus rex (Witmer et al. 2008); (L) Bubo virginianus (Witmer et al. 2008). † denotes extinct taxa. Phylogeny following Nesbitt (2011) and Ezcurra (2016). Brain cavities not to scale.
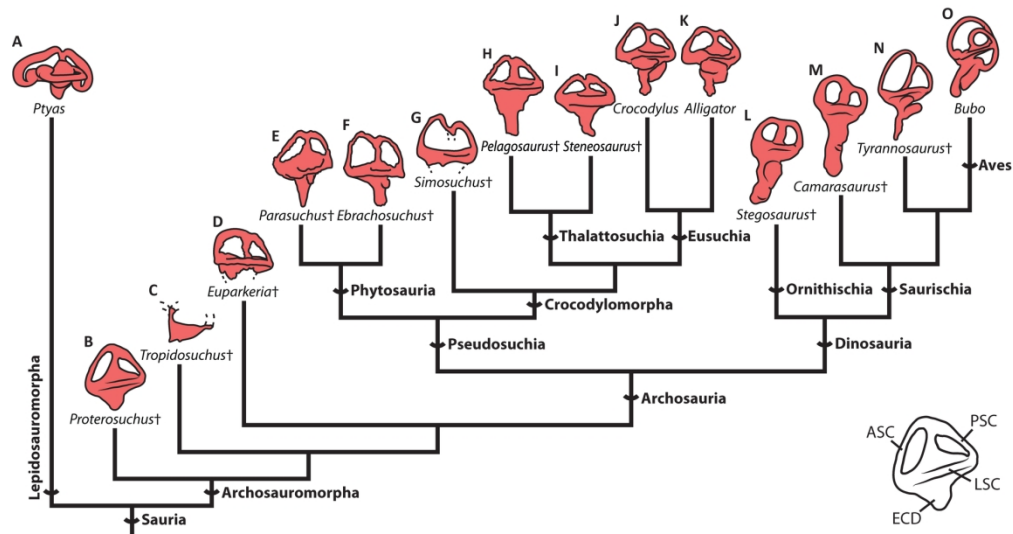
109x217mm (300 x 300 DPI)

FIG 11. Evolution of the endosseous labyrinth in Archosauriformes. Lateral view of the left labyrinth of archosauriforms redrawn from the literature. (A) snake Ptyas mucosa (reversed, Yi & Norell 2015); (B) Proterosuchus fergusi (this study); (C) proterochampsian Tropidosuchus romeri (reversed, Trotteyn & Paulina-Carabajal 2016); (D) Euparkeria capensis (reversed, Sobral et al. 2016); (E) Parasuchus angustifrons (retrodeformed, Lautenschlager & Butler 2016); (F) Ebrachosuchus neukami (retrodeformed, Lautenschlager & Butler 2016); (G) Simosuchus clarki (reversed, Kley 2010); (H) Pelagosaurus typus (Pierce et al. 2017); (I) Steneosaurus cf. gracilirostris (Brusatte et al. 2016); (J) Crocodylus johnstoni (Brusatte et al. 2016); (K) Alligator mississippiensis (Brusatte et al. 2016); (L) Stegosaurus stenops (Leahey et al. 2015); (M) Camarasaurus lentus (Witmer et al. 2008); (N) Tyrannosaurus rex (Witmer et al. 2008); (O) Bubo virginianus (Witmer et al. 2008). † denotes extinct taxa. Abbreviations: ASC, anterior semi-circular canal; ECD, endosseous cochlea duct; LSC, lateral semi-circular canal; PSC, posterior semi-circular canal. Phylogeny following Nesbitt (2011), Ezcurra (2016) and Leardi et al. (2017). Labyrinths not to scale.

166x87mm (300 x 300 DPI)